

FTUV/20-0302

IFIC/20-07

PenRed: An extensible and parallel Monte-Carlo framework for radiation transport based on PENELOPE

V. Giménez-Alventosa^a, V. Giménez Gómez^b, S. Oliver^c

^a*Instituto de Instrumentación para Imagen Molecular (I3M)*

Centro mixto CSIC - Universitat Politècnica de València

Camí de Vera s/n, 46022, València, Spain

^b*Departament de Física Teòrica and IFIC*

Universitat de València-CSIC

Dr. Moliner, 50, 46100, Burjassot, València, Spain

^c*Instituto de Seguridad Industrial, Radiofísica y Medioambiental (ISIRYM)*

Universitat Politècnica de València

Camí de Vera s/n, 46022, València, Spain

Abstract

Monte Carlo methods provide detailed and accurate results for radiation transport simulations. Unfortunately, the high computational cost of these methods limits its usage in real-time applications, such as clinical treatment planning. Moreover, existing computer codes do not provide a methodology for adapting these kind of simulations to specific problems without advanced knowledge of the corresponding code system, and this restricts their applicability. To help solve these current limitations, we present PenRed, a general-purpose, stand-alone and extensible framework code based on PENELOPE for parallel Monte Carlo simulations of electron-photon transport through matter. It has been implemented in C++ programming language and takes advantage of modern object-oriented technologies. In addition, PenRed offers the capability to read and process DICOM images on which it can construct and simulate voxelized geometries so as to facilitate its usage in medical applications. Our framework has been successfully tested against the original PENELOPE Fortran code.

Keywords: Radiation transport, Monte Carlo simulation, Electron-photon showers, Parallel computing, MPI, Medical physics

1. PROGRAM SUMMARY

Program title: PenRed: Parallel Engine for Radiation Energy Deposition.

Licensing provision: GNU Affero General Public License (AGPL).

Programming language: C++ standard 2011.

Nature of problem: Monte Carlo simulations usually require a huge amount of computation time to achieve low statistical uncertainties. In addition, many applications necessitate particular characteristics or the extraction of specific quantities from the simulation. However, most available Monte Carlo codes do not provide an efficient parallel and truly modular structure which allows users to easily customise their code to suit their needs without an in-depth knowledge of the code system.

Solution method: PenRed is a fully parallel, modular and customizable framework for Monte Carlo simulations of the passage of radiation through matter. It is based on the PENELOPE [1] code system, from which inherits its unique physics models and tracking algorithms for charged particles. PenRed has been coded in C++ following an object-oriented programming paradigm restricted to the C++11 standard. Our engine implements parallelism via a double approach: on the one hand, by using standard C++ threads for shared memory, improving the access and usage of the memory, and, on the other hand, via the MPI standard for distributed memory infrastructures. Notice that both kinds of parallelism can be combined together in the same simulation. In addition, PenRed provides a modular structure with methods designed to easily extend its functionality. Thus, users can create their own independent modules to adapt our engine to their needs without changing the existing modules. Furthermore, user extensions will take advantage of the built-in parallelism without any extra effort or knowledge of parallel programming.

Additional comments including Restrictions and Unusual features:

PenRed has been compiled in linux systems with `g++` of GCC versions 4.8.5, 7.3.1, 8.3.1 and 9; clang version 3.4.2 and intel C++ compiler (`icc`) version 19.0.5.281. Since it is a C++11-standard compliant code, PenRed should be able to compile with any compiler with C++11 support. In addition, if the code is compiled without MPI support, it does not require any non standard library. To enable MPI capabilities, the user needs to install whatever available MPI implementation, such as openMPI [2] or mpich [3], which can be found in the repositories of any linux distribution. Finally, to provide DICOM processing support, PenRed can be optionally compiled using the dicom toolkit (dcmtk) [4] library. Thus, PenRed has only two optional dependencies, an MPI implementation and the dcmtk library.

References:

- [1] F. Salvat, penelope-2018: A code System for Monte Carlo Simulation of Electron and Photon Transport, OECD/NEA Data Bank, Issy-les-Moulineaux, France, 2019, available from <http://www.nea.fr/lists/penelope.html>
- [2] Graham R.L., Woodall T.S., Squyres J.M. (2006) Open MPI: A Flexible High Performance MPI. In: Wyrzykowski R., Dongarra J., Meyer N., Waśniewski J. (eds) Parallel Processing and Applied Mathematics. PPAM 2005. Lecture Notes in Computer Science, vol 3911. Springer, Berlin, Heidelberg
- [3] William Gropp. 2002. MPICH2: A New Start for MPI Implementations. In Proceedings of the 9th European PVM/MPI Users' Group Meeting on Recent Advances in Parallel Virtual Machine and Message Passing Interface. Springer-Verlag, Berlin, Heidelberg, 7.
- [4] DCMTK, <https://github.com/DCMTK/dcmtk>, accessed: 2019-09-28

2. Introduction

Monte-Carlo (MC) methods are widely used in most scientific applications which involve radiation transport simulations, including electron microscopy and microanalysis, x-ray fluorescence, detector characterisation, radiation metrology, dosimetry and radiotherapy, among others. MC codes provide a detailed and accurate method for the calculation of absorbed dose in heterogeneous and complex systems such as the human body whereby are considered as the gold standard for this kind of calculus. One example is the simulation of radiotherapy treatments or instrumentation, such as brachytherapy, where MC is considered as one of the Model-Based Dose Calculations Algorithms recommended for clinical applications [1] instead of the current methods used in clinical practice based on approximations and model simplifications [2].

Among the most used techniques for cancer treatment, radiotherapy has become widely used, alone or combined with other techniques. This one consists in irradiating the cancerous region with ionising radiation to kill the disease preserving the healthy tissues. Taking into account that last National Cancer Institute survey concludes that the percentage of men and women that will be diagnosed with a cancer of any type during their lifetime is, approximately 39.3% [3] and that the 32.9% of diagnosed cancer ends in death in less than 5 years, any improvement in cancer diagnostics and treatment will have a great impact in the health of the society. MC codes have an important role in that way. On a conventional radiotherapy treatment planning, physicists and physicians determine the amount of dose, defined as imparted energy per unit mass, required to kill the injured zone avoiding to damage healthy tissues. For that planning, in addition to image techniques to locate the disease, radiation transport models to estimate the dose deposition across the patient are required. However, this calculus with MC codes implies huge computational effort with

long execution times, which makes difficult their usage for clinical purposes. Therefore, in practice simplified models are used, changing accuracy for speed.

This fact highlights the need of a fast parallel code for MC based radiation transport simulations which could run on modern computer architectures and take advantage of all the available resources. Moreover, as treatments evolve continuously, the code must be sufficiently flexible to incorporate new modules to allow simulations of future treatments. In addition, it must natively handle medical images in order to permit an individualised treatment planning. To meet these needs, this work presents PenRed (Parallel ENgine for Radiation Energy Deposition), a complete C++ framework, limited to C++11 standard, which provides a parallel and extensible environment for general-purpose MC simulations of the transport of electron and photon through matter. It incorporates a translated and restructured version of the physics models, particle tracking and sampling methods of the original PENELOPE [4] Fortran code system.

Our aim is to create an fully optimised, easily extensible and parallel framework for generic radiation transport simulations. In that way, PenRed is intended to be our first step towards employing MC codes in clinical routine practice. This would enable to use accurate models for medical treatment planings by improving the execution speed.

Although we focus on medical physics, it is important to remark that the new code introduced here is a general-purpose framework which can be used for other MC based applications such as particle accelerators, space engineering, radiation protection or industrial projects.

PenRed is free, distributed as open source software under the GPLA v3 license, and it can be found at GitHub [5].

The present article is organised as follows. Section 3 gives the state of the art of the current MC codes and describes the physics and interaction models of PENELOPE on which PenRed is based. In section 4, the PenRed capabilities are discussed. In section 5, the test results which ensure that our framework fully reproduces the original PENELOPE results are presented. Moreover, some additional test results which validate novel capabilities of PenRed are also described. Finally, section 6 contains our conclusions and future development plan for PenRed.

3. State of the art

Nowadays there exist several Monte Carlo based codes to perform simulations of ionising radiation transport, such as PENELOPE [6, 7], GEANT4 [8], EGS5 [9, 10, 11], MCNP [12] and FLUKA [13]. Among them, we choose PENELOPE because accurately handles the physics of electrons, photons and positrons in medical physics energy ranges, implements a better electromagnetic formalism for electrons and positrons, is free and open source, and its source code is relatively simple compared with other Monte Carlo codes.

PENELOPE is a general-purpose Fortran code system for the Monte Carlo simulation of coupled electron-photon transport that simulates electron, positron

and photon showers in material systems consisting of homogeneous bodies with arbitrary chemical compositions, within the energy range from 50 eV to 1 GeV. As we will briefly discuss below, PENELOPE implements the most reliable interaction models currently available. Moreover, its results have been tested against experimental data and the agreement has been very good [14]. In addition, it includes three packages with generic tools for random sampling, implementations of variance-reduction techniques and subroutines for automatic tracking of particles within material systems consisting of homogeneous bodies limited by quadric surfaces.

3.1. PENELOPE physics and interaction models

In this section we will briefly describe the physics and interaction models of the PENELOPE code.

In order to avoid diffraction effects and simplify the angular dependence of the interactions, the radiation (electrons, positrons and photons) is assumed to propagate in amorphous, homogeneous and isotropic materials. During its propagation, the radiation interacts with the atoms of the material through specific mechanisms, to be described below. The important thing is that the angular deflection and energy loss of the particles after the scattering are described by differential cross sections (DCS hereafter), which are a measure of the quantum-mechanical probability of the different outcomes. The state of each transported particle is characterised by its energy, position and direction of motion. The simulation is made of particle histories which are random sequence of free flights and interactions, generated by the physics subroutines. As a probabilistic process, the length of the free flight, the type of interaction, the energy loss and the angular deflection are sampled directly from the corresponding DCS or from derived quantities. A particle history ends when its energy is lower than a user-defined absorption energy or it escapes from the material system. The tracking subroutines take care of possible secondary particles produced during the scattering or in the relaxation of atoms after inner-shell ionisations. Secondary particles are stored in a LIFO stack depending on their type and are simulated after the absorption of the primary particle.

One of the most relevant and distinguishing characteristics of PENELOPE is the usage of a combination of accurate numerical databases and reliable analytical atomic differential cross sections for the different interaction mechanisms, valid for relatively low energies. The corresponding total cross sections are calculated by the function SUMGA which performs a rapid numerical quadrature. Molecular cross sections and those for mixtures and compounds are approximated by the incoherent sum of the atomic cross sections of their atoms. This so-called Bragg's additivity approximation is valid provided that coherent interference effects are negligible.

The use of reliable DCS is very important in Monte Carlo simulations. Since its first release, 1996, the author, F. Salvat, has added many refinements in order to improve both the accuracy and stability under variations of the user-defined simulation parameters. The database of PENELOPE, provided in the package, consists of 995 ASCII files which include tables of the numerical values

of physical properties, relaxation data, DCS, total cross sections and some other energy-dependent quantities, like first and second transport cross sections; one for each element from hydrogen to einsteinium, at fixed grids of particle energies and scattering angles. The energy grid spans the range from 50 eV to 1 GeV. For energies above ~ 1 keV, the tables are accurate to within a few per cent, whereas for lower energies the uncertainties are much larger because the DCS are not well known due their strong dependence on the state of aggregation. However, in inelastic interactions of electrons and positrons the aggregation state is approximately taken into account through the mass density and mean excitation energy of the material.

An auxiliary program, material.f, extracts the physical information about each material in the simulation from the database and creates a material data file, which is read by PENELOPE in the initialisation phase. After reading the DCS from the database files, PENELOPE produces a table for a denser logarithmic grid by natural cubic spline interpolation/extrapolation in $\ln E$, which is stored in memory. The energy grid spans the full energy range considered in the simulation and allows accurate and fast linear log-log interpolations of the DCS.

A catalogue of the physics and interaction models considered in PENELOPE and a schematic description of the corresponding differential cross sections follows. A complete discussion of these items can be found in the PENELOPE manual [7] and also in [15] and the original references therein.

Electron-positron interactions

1. Elastic scattering of electrons and positrons.

In elastic interactions the initial and final quantum states of the target (atom or molecule) are the same, usually the ground state. These interactions change the direction of motion of the projectile and there is also a certain energy transfer from the projectile to the target, which causes the recoil of the latter. In PENELOPE, they are simulated using numerical DCS obtained with the program ELSEPA [16, 17] by using the relativistic Dirac partial-wave method.

2. Inelastic collisions of electrons and positrons.

In inelastic interactions the target is brought to an excited state, i.e. some of the projectile's kinetic energy is taken up by the atomic electrons. The projectile also changes its direction of motion, but to a lesser degree than in the case of elastic collisions. PENELOPE simulates them by means of the plane-wave Born DCS obtained from the Sternheimer–Liljequist generalized oscillator strength (GOS) model [18, 19], including the density-effect correction. The resonance energies are scaled in order to reproduce the mean excitation energy recommended in the ICRU Report 37, [20]. As a consequence, collision stopping powers calculated from this model agree closely with those from the ICRU Report 37.

3. Inner-shell ionisation by electron and positron impact.

PENELOPE simulates inner-shell ionization (K shell and L, M and N subshells) and the subsequent emission of fluorescent radiation, i.e., Auger electrons and characteristic x rays, as a real inelastic collisions with numerical total cross sections calculated by Bote and Salvat [21] using the distorted-wave (first) Born approximation (DWBA) with the Dirac-Hartree-Fock-Slater self-consistent potential [22]. This is accomplished by setting the total cross section for collisions with electrons in each inner shell equal to the DWBA cross section, and by renormalising the total cross sections of outer shells so as to keep the value of the collision stopping power unaltered. The energy loss and the angular deflection are sampled from the Liljequist-Sternheimer GOS model. This approach has the advantage of yielding a nearly correct number of ionizations per unit path length, without altering the modeling of inelastic collisions.

4. Bremsstrahlung emission by electrons and positrons.

The emission of bremsstrahlung photons takes place when the projectile is accelerated in the electrostatic field of the target atom. For electrons and positrons, this becomes the dominant energy loss mechanism for high energies. The energy of the emitted photon is sampled from numerical energy-loss spectra derived from the scaled cross-section tables of Seltzer and Berger [23, 24]. The angular distribution of emitted photons is simulated using an analytical expression [25] with parameters determined by fitting angular distributions calculated with the program BREMS of Poskus [26].

5. Positron annihilation.

In PENELOPE the annihilation of an electron and a positron is simulated by using the Heitler DCS [27] for in-flight two-photon annihilation with free electrons at rest. Since binding effects of the target electron are not considered, one-photon annihilation is not taken into account.

Photon interactions

1. Coherent (Rayleigh) scattering of photons.

In coherent scattering, photons are scattered by bound atomic electrons and interfere quantum-mechanically in such a way that there is no excitation of the target atom. Thus, the energies of incoming and outgoing photons are the same. In PENELOPE it is simulated by means of DCS calculated using non-relativistic perturbation theory in the Born approximation with form factors and effective anomalous scattering factors [28] obtained from EPDL97 [29]. PENELOPE can also simulate Rayleigh scattering of polarised photons described by the Stokes parameters.

2. Incoherent (Compton) scattering of photons.

In incoherent scattering, a photon collides with an atomic electron

that absorbs it and emits a secondary photon with a different energy and direction of motion. This process is simulated using DCS calculated from the relativistic impulse approximation with analytical one-electron Compton profiles, which takes into account both binding effects and Doppler broadening [30]. PENELOPE can also simulate Compton scattering of polarised photons described by the Stokes parameters.

3. Photoelectric absorption of photons.

In this process, a photon is absorbed by the target atom which makes a transition to an excited state. This interaction is simulated through DCS calculated with the program PHOTACS by using conventional first-order perturbation theory [31] and including a screening correction proposed by Pratt [32].

4. Electron-positron pair production.

If a photon has energy above a certain threshold, it can be absorbed in the electromagnetic field of a nucleus or electron and its energy converted to particle mass conserving energy, momentum and electric charge. If the absorption occurs near a nucleus an electron-positron pair is created, whereas if it occurs in the vicinity of an electron, the target recoils and three particles are observed (triplet production). In PENELOPE, the total cross sections for pair and triplet production are obtained from the XCOM program [33]. The initial kinetic energies are sampled from the screening and Coulomb corrected Bethe-Heitler DCS.

Atomic relaxation

In PENELOPE, hard inelastic collisions with atomic inner shells, photoelectric absorption and Compton scattering are assumed to ionise the target atom and the relaxation of the resulting vacancies produces the isotropic emission of characteristic x-rays and Auger electrons. These are simulated by the RELAX subroutine, using the transition probabilities of the vacancies towards outer shells and the energies of Auger electrons given in the Evaluated Atomic Data Library of Perkins et al. [34]. The energies of x-ray lines are taken from [35] and [36].

The PENELOPE manual contains a detailed description of the sampling algorithms used to simulate the above mentioned interactions from the corresponding DCS. Briefly, continuous distributions are sampled employing RITA (Rational Inverse Transform with Aliasing) while to sample discrete distributions with a large number of outcomes, the Walker's aliasing method is used [37].

3.2. *Class II scheme and simulation parameters*

The tracking algorithm of PENELOPE is a mixed or class II one which depends on certain angle and energy cutoffs. A proper selection of these mixed

Parameter	Description	Range	Recommended values
E_{abs}	Particle absorption energies for each material in eV	$E_{abs} \geq 50$ eV	range(E_{abs}) < L_{bin} scan E_{abs} parameter space via short runs
C_1	Maximum average angular deflection	[0, 0.2]	~ 0.05 scan C_1 parameter space via short runs
C_2	Maximum average fractional energy loss	[0, 0.2]	~ 0.05 scan C_2 parameter space via short runs
W_{cc}	Energy-loss threshold in eV for hard inelastic collisions	[0, $E_{abs}(e^-)$]	$\min(5 \text{ keV}, \frac{1}{100}E)$
W_{cr}	Energy-loss threshold in eV for hard bremsstrahlung radiation	[10 eV, $E_{abs}(\gamma)$] For $W_{cr} < 0$ soft radiation is switched off	$\min(5 \text{ keV}, \frac{1}{100}E)$
s_{max}	Maximum step length in cm	$s_{max} \geq 0$	$\sim 1/10$ minimal body thickness

Table 1: User parameters determining the accuracy and speed of simulations in PENELOPE. The recommended values correspond to an accuracy-speed tradeoff, by their influence should be studied case by case. Faster simulations can be obtained using larger values of the parameters but at the price of a possible loss of accuracy and reliability. See the text for details.

simulation parameters may substantially improve the efficiency of the simulation. In this way, permissible statistical uncertainties, that severely limit the usefulness of Monte Carlo simulations in practical applications, can be reached much faster. In this section, we briefly describe the class II scheme and some practical rules for the election of the simulation parameters in PENELOPE, summarised in Table 1. The same conclusions apply to our code PenRed.

In PENELOPE, like in most Monte Carlo codes, the tracking of particles is discontinued when their kinetic energies fall below certain user-defined absorption energies, E_{abs} , set by the user for each material in the geometry. Positrons annihilate by emission of two photons when absorbed. It is worth mentioning that both the number of secondary particles and the simulation time increase with the decreasing of E_{abs} , being 50 eV the lowest absorption energy allowed by the program. Moreover, when the user is interested in the spatial distribution of absorbed energy, for example in dosimetric calculations, the absorption energies should be selected so that a particle with energy equal to E_{abs} deposits all its energy within distances much shorter than the thickness of the volume

bins used to tally this quantity. Otherwise, it is recommended to scan the effect of the E_{abs} in the results by running short simulations with increasing values of the absorption energies [7].

As it is said in the previous section, photons, being neutral particles, are simulated interaction by interaction in a chronological succession, i.e. in a detailed or analogue scheme. Electron and positrons, by contrast, are charged particles and therefore their simulation is much more difficult due to the large number of interactions between them and atoms that take place until they are absorbed. Thus, a detailed simulation of electrons and positrons is only feasible when the number of interactions is sufficiently small, for example, for low kinetic energies or thin foils. One way around this problem is to estimate the combined effect of all the interactions that occur along each of the many steps of preselected length in which the particle track can be decomposed [38]. The steps must be long enough to ensure a large the number of interactions along it. Both the global energy loss and angular deflection in a step are sampled from approximate multiple scattering theories [39]. This technique is referred to as condensed simulation or class I scheme.

However, class I schemes have significant drawbacks. Firstly, the distribution of spatial displacements after a given path length is partially unknown. Secondly, since the multiple scattering theories are valid in an homogeneous and infinite medium, the distance to all the nearest interfaces must be calculated in order to keep the step length small enough not to change the material where the particle propagates. Therefore, when a particle approaches an interface the step length must be progressively reduced, which directly conflicts with a pre-selected step length and restricts the objects which can be efficiently modelled. A strategy employed by some Class I codes, like EGSnrc [11, 40], consists in switching to single scattering mode whenever the particle is in the vicinity of an interface.

A more practical solution are the so-called mixed or class II schemes. The crucial observation is that the DCS for interactions of high-energy charged particles decrease quickly with both increasing energy loss W and polar scattering angle θ or angular deflection $\mu \equiv (1 - \cos \theta)/2$ (roughly as μ^{-2} for elastic interactions, $\mu^{-2} W^{-2}$ for inelastic collisions and as W^{-1} for bremsstrahlung emission). This fact can be exploited to split the interactions into two categories, soft and hard, which can be simulated differently to diminish the effective number of interactions. To this end, two energy-dependent cutoffs are introduced: W_c , for the energy loss and θ_c , for the polar scattering angle. On the one hand, the expected small number of interactions with energy loss and scattering polar angle larger than W_c and θ_c , respectively, are called hard, treated discretely and simulated individually by random sampling from the corresponding restricted DCS. On the other hand, interactions with W and θ lower than their cutoffs, the large majority of the processes, are called soft and their accumulated angular deflection in a step between two successive hard interactions are accounted for approximate multiple-scattering distributions valid beyond the continuous slowing down approximation (CSDA assumes that the particle's energy loss is continuous with a rate equal to the stopping power). The spatial displacement

at the end of a step is determined by using the so-called random-hinge algorithm [41]. The combined effect of all the soft interactions that occur between two consecutive hard collisions is accounted for by means of a single artificial soft interaction, a hinge, in which the particle is deflected and its energy is reduced. Notice that the secondary particles produced by soft collisions are disregarded. The position of the hinge is sampled uniformly along the step and after the hinge the particle moves the remaining distance in the new direction. In this way, each step is divided into two segments. This algorithm allows a very important simplification of the simulation code and has been shown to provide accurate values of relevant angular and spatial moments. Moreover, in the vicinity of interfaces separating two different materials, the step is simply truncated. For further details, the reader is referred to the excellent manual of PENELOPE [7] and to a general description of class II algorithms [42].

In PENELOPE, but unlike most other general-purpose Monte Carlo codes, the generation of electron and positron tracks is systematically performed by means of a mixed (class II) algorithm for all interactions. This scheme is more accurate and numerically stable than purely condensed (class I) schemes.

The energy-dependent cutoffs W_c and θ_c are determined internally using four energy-independent simulation parameters specified by the user for each material in the geometry. It is important to note that both the accuracy and efficiency of the simulation strongly depend on these parameters.

For energy-loss events, two simulation parameters should be defined in eV: W_{cc} , for inelastic collisions, and W_{cr} , for bremsstrahlung radiative events, such that processes with W lower than W_{cc} or W_{cr} are considered soft interactions. Internally, the values of these parameters are used to compute the corresponding hard mean free paths, i.e. the average distance between two hard energy-loss interactions. The threshold energies W_{cc} and W_{cr} have a visible effect on simulated energy spectra and hence they both should be smaller than the energy bin width, but in this case they have a mild effect on the accuracy of the results. Due to the rapidly decreasing dependence on W of the inelastic and bremsstrahlung DCS, they also have a weak effect on the simulation speed for energies higher than about 100 keV. However, W_{cc} and W_{cr} should not be too large. Firstly, because for consistency they must be smaller than the corresponding E_{abs} in a given material. And secondly, because larger values imply longer steps between hard interactions and thus a smaller number of them, what could affect the reliability of the approximate description of energy-straggling distributions (see below). The recommended value for these cutoff energies is the lower of 5 keV and one hundredth of the initial energy of primary particles [7]. The reason for this rule is that in this case the number of hard interactions is statistically sufficient and the simulation speed remains practically constant when they are given larger values. Finally, notice that W_{cr} , unlike W_{cc} , cannot be set to zero because the Bremsstrahlung emission DCS diverges at zero photon energy. In order to perform almost detailed simulations of radiative events, a negative value of W_{cr} can be defined so that W_{cr} is internally set to 10 eV and the emission of photons with lower energy disregarded (see below).

The mean free path between two hard elastic events, $\lambda_{el}^{(h)}$, which in turn fixes the cutoff deflection angle θ_c , which separates soft and hard elastic interactions, is determined by two user parameters, C_1 and C_2 . The former sets an upper limit to the average angular deflection at the end of a step of length equal to the hard elastic mean free path, $1 - \langle \cos \theta \rangle \leq C_1$. The latter limits the average fractional energy loss along the step, $\langle E_0 - E \rangle \leq C_2 E_0$. Provided the values of C_1 and C_2 are not too large, they have a very low effect on the accuracy of the results but it is worth noting that an increase of these parameters results in an increase in both $\lambda_{el}^{(h)}$ and θ_c and hence affect the computer time needed to simulate each electron and positron track. Moreover, they act on different energy domains. In fact, C_1 influences the simulation speed only at intermediate energies, typically less than 10 MeV, where $\lambda_{el}^{(h)}$ is almost insensitive to C_2 . However, at high energies, the simulation speed is practically controlled by C_2 . At low energies, say less than 10 keV, the hard elastic mean free path is equal to the elastic one, $\theta_c = 0$ and the simulation is purely detailed. The recommended values of C_1 and C_2 are small, typically in the range between 0 and 0.05, without exceeding 0.2, but larger values can be adopted after a study of their effect on the accuracy and speed of the simulation by performing short test runs.

In class II scheme, the angular deflection and lateral displacement due to soft interactions along a step of length s , must be sampled on the fly, in principle, from the exact Lewis multiple-scattering distribution [39][43, 44]. However, the latter is not appropriate for Monte Carlo simulations, since it is a Legendre expansion which converges very slowly and the sum varies rapidly with s . A possible solution to this problem is to realise that for small angles the multiple-scattering distribution does not differ substantially from a Gaussian distribution with known mean and variance [45][41]. Unfortunately, the small-angle approximation is only applicable in a few cases. A more practical approach consists in exploiting the fact that the angular distribution become nearly Gaussian, i.e. it is accurately determined by its mean and variance only, when the particle undergoes about ten or more interactions. Therefore, in this case, it is not necessary to use the exact distribution because a simpler artificial distribution, with the correct mean and variance, can be employed instead (see chapter 4 of the PENELOPE manual). A similar method is used to simulate soft energy losses. Indeed, the multiple-scattering distribution of the energy loss satisfies the Landau transport equation [46], but an exact solution to this equation is not necessary if the number of soft interactions is large enough. In this case, the energy loss distribution is again nearly Gaussian, with known and calculable mean and variance, and other details of the distribution are irrelevant. Therefore, a simpler, artificial but equivalent energy loss distribution, suitable for Monte Carlo simulations, can be used to sample the energy loss in a step due to soft inelastic interactions (see Chapter 4 of the PENELOPE manual). In this way, PENELOPE, simulates the combined effect of all soft elastic and inelastic collisions that occur between two hard interactions.

In critical geometries, for example, for thin bodies or backscattering, the condition for the applicability of the approximate energy loss and angular de-

flection distributions could not be met. However, by limiting the step length by defining the user parameter s_{max} , the maximum step length, it is possible to guarantee that the number of steps per primary track within the material is large enough to wash out the details of the artificial distributions. The reliability of a simulation rests on this condition. Moreover, the quantities that define the multiple-scattering distributions, like the hard and transport mean free paths, depend on the energy of the particle, which decreases along a step due to the soft collisions. In order to properly take into account this variation in our class II scheme, the energy loss due to soft interactions must be bounded. In Penelope, this is done internally by setting the parameter s_{max} equal to four times the hard mean free path so that if the sampled step length is longer than s_{max} , it is truncated by imposing a so-called delta interaction which does nothing but stops the particle and the program flow [40]. Therefore, s_{max} only needs to be modified in the case of thin bodies and a value of the order of one tenth of the minimal thickness of the body is usually adequate [7].

As it is said before, the parameters E_{abs} , C_1 , C_2 , W_{cc} , W_{cr} and s_{max} determine the simulation speed in such a way that the simulation slows down if any of them is reduced; i.e. the larger their values, the faster will be the simulation because more soft interactions are merged together. However, they also determine the accuracy of the simulation so that for obtaining precise results, these parameters should have small values, for example, ~ 0.01 for C_1 and C_2 . Since the threshold energies W_{cc} and W_{cr} mainly affect the simulated energy distribution, too large values could distort it. In practice, the energy distributions are insensitive to these cutoff energies provided they are smaller than the desired energy resolution.

An important advantage of this class II scheme is that it produces a fully analogue simulation, nominally exact, of elastic and inelastic collisions, in the limiting case when the parameters W_{cc} , C_1 and C_2 are set to zero. As mentioned above, an almost detailed simulation of radiative events is obtained by setting a negative value of W_{cr} , for example $W_{cr} = -10$ eV. Therefore, the user can verify both the accuracy and stability under changing the values of the user parameters by comparing simulation results with those of a detailed simulation. It has been verified that the results are nearly insensitive to the user parameters provided their values are not too large.

3.3. PENELOPE Main

PENELOPE in itself is not a simulation program that can be used for Monte Carlo simulations. It merely provides the code necessary to simulate the transport of a particle inside materials. It is the responsibility of the user to create a code from the sources which governs the simulation, keeps track of secondary particles, monitors the deposited energy, etc; i.e. a MAIN program. Therefore, it takes some time to write a new simulation program for a specific simulation problem. The new code has to be tested and verified and that can also take significant time.

In principle, the user should provide a MAIN program for each specific geometry. However, the PENELOPE distribution package includes various examples

of MAIN programs for simple geometries (slab and cylindrical) and for general quadric geometries, with limited scoring and variance reduction options, the so-called PENMAIN. This is a generic main program that performs simulations of electron-photon transport in complex material structures. PENMAIN is devised to allow occasional users to employ PENELOPE without having to write their own main program. The geometry of the material system is described by means of the package PENGEOM, which is able to handle complicated geometries very efficiently. The operation of PENMAIN is completely controlled from the input data files. Although it is impossible to cover all possible cases with a "closed" program, PENMAIN is flexible enough to solve a broad class of practical problems. The reader may consult the PENELOPE manual [7] for a detailed discussion of the precise rules to create geometry and input data files.

In the rest of this section, we touch on some practical aspects of the operation of the PENELOPE system. We start with a brief description of the general guidelines on how to run the code:

1. Write your own or modify the provided Main program in Fortran.
2. Prepare the necessary ASCII input data files to describe the geometry, the corresponding materials and the physical characteristics of the experimental arrangement to be simulated.
 - The program `material.f` is used for the material data file preparation.
 - Auxiliary programs such as `gview2d` and `gview3d` may be used to check the correctness of the geometry data file.
3. Compile and link the Main program with the PENELOPE subroutines.
4. Run the executable with the input data files.

A dump/resume option allows the user to stop the simulation at any time and to resume it from the last dumping point in a completely consistent way. The program can also write simulation results in the output files at regular time intervals. This option is useful to check the progress of long simulations. It also allows running the program with a long execution time and stopping it when the required statistical uncertainty has been reached.

The input data files that the user has to prepare are the following:

- The `file.mat` to describe the materials used in the system.
- The `file.geo` to describe the geometry of the system.
- The `file.in` to initiate various parameters (number of showers, detectors used, source type and energy, number of bins, etc)

Simulation results, like fluency, dose or absorbed energy, are computed by means of the corresponding detectors. Several types of detectors are included in the PENELOPE code in order to record various parameters and distributions:

- Impact detectors, which keep track of the main characteristics of the particles coming in the detector.
- Energy deposition detectors, which registers the energy of a particle that is deposited in the detector.

- Dose enclosure, which record the dose distribution within a specific system volume.

The physical results of the simulation are saved in several output data files. Two general types of output files are produced by PENELOPE:

- Files with the main parameters of the simulation and several useful information such as average values of physical quantities (e.g. `penmain.dat`).
- Files with space or energy distributions for various parameters, such as energy distribution of the deposited energy on a detector (e.g. `pm_spc_end-det.dat`).

Finally, the PENELOPE package includes some auxiliary programs and scripts such as:

- The program `shower.f` for the visual representation of the simulation in real time.
- The program `tables.f` for the creation of tables of energy dependent quantities such as linear attenuation coefficients, etc.
- A set of `gnuplot` [47] scripts for the graphical representation of the energy dependent quantities.

3.4. *Shortcomings of PENELOPE*

Unfortunately, despite of all the great features implemented in the PENELOPE code, it has some shortcomings which prevent it from being used in fast, large-scale and time-consuming applications, such as clinical high-precision dosimetry based on medical imaging and other aspects of medical radiation physics, among others, which are the main aim of this work. The major limitations of the PENELOPE system are as follows. Firstly, PENELOPE has been written mostly in Fortran 77, a somewhat old-fashioned programming language. As a consequence, it has been becoming increasingly difficult to maintain and optimise. For example, the code is filled with goto instructions, which is not object oriented programming and very hard to port to acceleration hardware such as GPGPUs. Secondly, PENELOPE and its provided main program are not easily extensible to other particles, sources, geometries or tallies needed by the users. Thirdly, it does not support multithreading nor multiprocessing technologies for parallel execution. This is a crucial requirement for a Monte Carlo simulation code to be systematically used in everyday clinical practice. Finally, reading and processing of DICOM clinical images is also not supported. However, this should be a key feature of any simulation code in medical physics.

4. Material and Methods

In order to overcome the limitations enumerated in section 3.4, we have created PenRed. The goals behind the development of this software for Monte

Carlo simulations of the passage of radiation through matter are extensibility, easy of maintenance, transparency of the design, modularity and specially performance. Since we know that an Object Oriented (OO) approach facilitates the achievement of these objectives, PenRed has been written in C++ using modern object-oriented techniques. The C++ is the de facto standard for OO programming, has a high performance, is a highly optimizable language, is well known in the scientific community and has big commercial support. These features allow us to create a Monte Carlo framework easy to maintain and optimise, completely modular and easily extensible. Therefore, the user of PenRed must know some elements of C++ in order to get the best from this software. In addition, PenRed supports both multithreading and multiprocessing and is capable of processing DICOM images using the DICOM toolkit (DCMTK) library [48]. Our framework includes a complete rewriting of the PENELOPE Fortran physics functions using advanced C++ classes and modern object-oriented techniques. Consequently, the whole discussion and conclusions on PENELOPE physics and simulation parameters of section 3 above are inherited by the physics implemented in PenRed.

4.1. PenRed tracking

As discussed in section 3.2, a strong simplification of the tracking of charged particles in Class II schemes can be achieved by using the random hinge method. Indeed, in this way the simulation of all kinds of particles (photons, electrons and positrons) follows the usual detailed procedure, i.e. the transported particles move in straight steps, and the energy and direction of motion change only through discrete events, hard interactions and hinges, simulated in chronological succession in each history. The basic algorithm for the generation of random histories is shown in figure 1, where colours represent the different PenRed components that handle each step of a detailed simulation. Each component type (geometry, particle, etc.) has a predefined and common interface shared with all components of the same type. Thus new components of any type can be added so that they will be compatible with the existing ones without having to modify their source code. Moreover, depending on the main program structure, it is possible to add new components without modifying the main program code, as we will see below.

In this section we will briefly describe the basic simulation algorithm depicted in figure 1, which is a simplified instance of the implementation of the main program provided in the PenRed package. A complete detailed description of the PenRed main program can be found in the documentation. Firstly, the program must initialise the databases required for the simulation, i.e. material, geometry and context information. Material and geometry databases store, respectively, the specific information for each material such as cross sections, ranges, etc. and the geometry where the particles move in the simulation. Both components are stored in the *context* class, which wraps all the constant information required by the simulation.

In addition, users commonly need a configurable method to initialise the states of the particles. A particle state is a data structure that contains all the

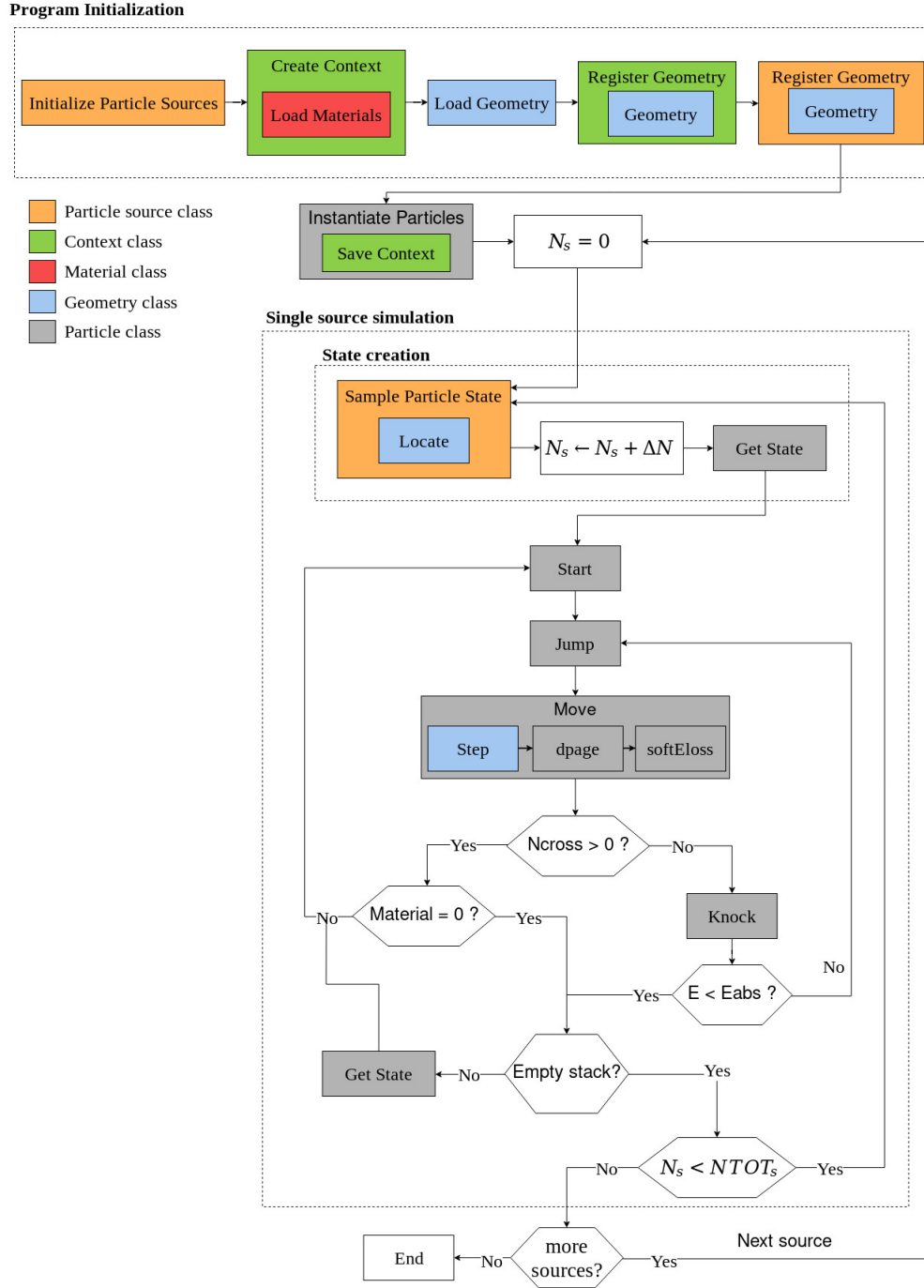


Figure 1: Basic flow diagram of the PenRed main program. For more details and a complete description of the flow chart, see the text.

necessary information to characterise a particle and its position in the geometry system. A basic state includes its position $\vec{r} = (X, Y, Z)$, energy E , direction of motion $\hat{d} = (U, V, W)$, particle age, geometry body and material indexes (IBODY and MAT, respectively) where the particle moves, statistical weight (WGHT) and particle label array (ILB[5]). The latter two state variables must be set to $WGHT = 1$ and $ILB[0] = 1$, respectively, for a primary particle. On the other hand, the body and material indexes depend on the geometry component, and must be assigned using the geometry method *locate*. This basic state can be extended to fit other particle needs. For example, to simulate PENELOPE polarised photons, we use an extended state with an active polarisation flag (IPOL), and three variables to specify their polarisation state by means of the Stokes parameters SP1, SP2 and SP3. Notice that a particle class contains a particle state, but a state is only a structure with the data listed above, but it is not a particle class itself. Thus, these states must be copied to particle instances to start the simulation, as we will explain below.

In order to generate particle states, PenRed uses the particle source class, which provides configurable methods to sample particle states. As we can see in figure 1, particle samplers register the geometry during the initialisation step. Therefore, particle sources can assign the body and material indexes to the particle state using the *locate* method. A more detailed information about particle state samplers can be found in section 4.2.2.

Once all databases have been loaded, the next step is to create the particle instances to be simulated. These are handled by a particle class which requires that a context be constructed and stored as a constant object to be accessible within all particle methods.

Since users can define multiple particle sources, the next stage is to begin a for-loop over all sources. Each iteration will finish when the number of simulated histories of the current source (N_s) reaches the required total number of histories ($NTOT_s$). Inside the body of this loop, the program uses the particle source component to sample the initial state of the next particle to be simulated. Notice that, in addition to the particle state, the sample function will return the shift of the history counter. In other words, an increment of 1 is not assumed because some samplers may create multiple states in the same history or skip more than one history between consecutive sample calls. Two examples of this are samplers that use splitting on primary particles or read particle states from a phase space file. Therefore, the new history counter is given by

$$N_s = N_s + \Delta N \quad (1)$$

At this point, a particle state ready to be simulated has been created. This state is set to the particle class to begin the simulation. Then, a call to the *start* method initialises the required variables depending on the particle type. After that, the simulation starts by calling the *jump* method, which calculates the step length (s) to the next interaction, i.e. the length of the next track step. As in PENELOPE, the distance s is set by random sampling from the exponential distribution $p(s) = \lambda_T^{-1} \exp(-s/\lambda_T)$, where λ_T is the total mean free path

for particles of energy E . To clarify this concept, consider for example that there are two interaction mechanisms with total cross sections σ_A and σ_B . The inverse mean free path associated with each mechanism is $\lambda_i^{-1} = N \sigma_i$, where $i = A, B$, and N the density of targets (atoms or molecules) in the material. Therefore, the inverse total mean free path, the interaction probability per unit of path length, is given by $\lambda_T^{-1} = \lambda_A^{-1} + \lambda_B^{-1}$. Finally, the sampling of s from $p(s)$ is done using ξ , a random number uniformly distributed in the interval $(0, 1)$, which is defined as $s = -\lambda_T \ln \xi$. As seen in section 3.2, for electrons and positrons, s will never exceed the value **DSMAX**, which is specified by the user for each material or body during the configuration. For photons, **DSMAX** has no effect. The rationale for the introduction of this parameter that limits the step length is discussed in section 3.2.

Once the distance to travel to the next interaction through the current material has been determined, the next step is to move the particle. To achieve this purpose, all particles have a method named *move*, which implementation is common to all particle types. Internally, the *move* method calls the geometry method *step*. Furthermore, it handles the particle age increment and the soft energy loss, which simplifies new particle implementation and usage. The *step* method of any geometry (quadric, voxel or other) must displace the particle from the current position $\vec{r} = (X, Y, Z)$ to the final position $\vec{r} + s \hat{d}$, a free flight of length s in the direction \hat{d} . However, this method must check if any interface will be crossed by the particle during its flight. Any change of material or detector is considered an interface. If this is the case, the particle is stopped at the first crossed interface and the output variable **NCROSS** incremented, i.e. it is set to a value greater than zero. Moreover, if, after entering a new material, this is void (**MAT** = 0), the step method must try to skip the void and move the particle to the next non-void material interface. If no non-void material can be found in the direction of propagation, the particle will be moved an “infinite” distance through the void region and it will leave the system. It is worth noting that if the initial material is the void, the particle is moved to the first region with **MAT** > 0, or leaves the system.

After the particle free flight, the value of **NCROSS** must be checked. A **NCROSS** = 0 means that the particle has not crossed any interface and thus the next step is to simulate an interaction or hinge with the material. The latter is handled by the *knock* particle method, where interaction or hinge selection, energy losses, modifications of the direction of motion and secondary particle generation are usually performed. Since after a call to the *knock* method the particle could lose energy, it is necessary to check whether its energy is below the absorption one. In such case, the particle is absorbed locally i.e. deposits all its remaining energy at the position \vec{r} . Otherwise, the flow returns to the *jump* step and the procedure is repeated until the particle crosses an interface or it is absorbed. It is important to bear in mind that the *jump* and *knock* methods must be called with an energy larger than the absorption one but lower than the maximum, in order to perform a correct interpolation of the cross sections. This condition must be verified at the start of a new primary or secondary track

by calling the particle method *start*.

On the other hand, a NCROSS greater than zero means that the particle has crossed an interface. If the material after crossing the interface is a non-void material, the flow must return to the *start* call to continue the simulation of the track in the new material. If the particle remains in a void region, it has escaped from the geometry system.

Regardless of whether the particle has escaped or has been absorbed, its track ends. The next step must be to check if there are any secondary particles to simulate. If this is the case, their states have been previously stored in particle state stacks. If the stacks are not empty, a stored state is set to the particle class and the flow returns to the *start* call. Otherwise, if the number of histories simulated (N_s) is lower than the target number of histories ($NTOT_s$), the program will return to the state sampling. However, if the number of simulated histories has reached the required number, the simulation of this source is considered finished. This loop will be repeated for every source specified in the input file to, finally, complete the simulation.

The algorithm described above performs the simulation of the radiation transport, but it does not extract any output data from it. To solve this problem, the main program must include some tallies to store the quantities of interest. The PenRed package includes several tallies and a mechanism to allow the user to create and integrate new tallies without any change in the main program nor in other components. These tallies are handled by a tally class, which basic functions will be briefly described below. However, a detailed description of all components can be found at the provided manual and examples.

The tally class has a set of methods that will be called automatically at different parts of the algorithm, where some relevant events take place, as can be seen in figure 2. Some of these methods are the following:

- **tally_beginSim**: Called when simulation begins.
- **tally_endSim**: Called when simulation ends.
- **tally_beginHist**: Called when a new history begins.
- **tally_endHist**: Called when a history ends, i.e. both the primary particle and all its secondary particles have been simulated.
- **tally_beginPart**: Called when a new particle simulation loop starts.
- **tally_endPart**: Called when a particle simulation loop ends, for both primary and secondary particles.
- **tally_Eloss**: Called when a particle loses energy locally. For example, when the particle interact with the material or is absorbed.
- **tally_step**: Called after a call to the *step* method during the particle simulation.
- **tally_interfCross**: Called when a particle crosses an interface.

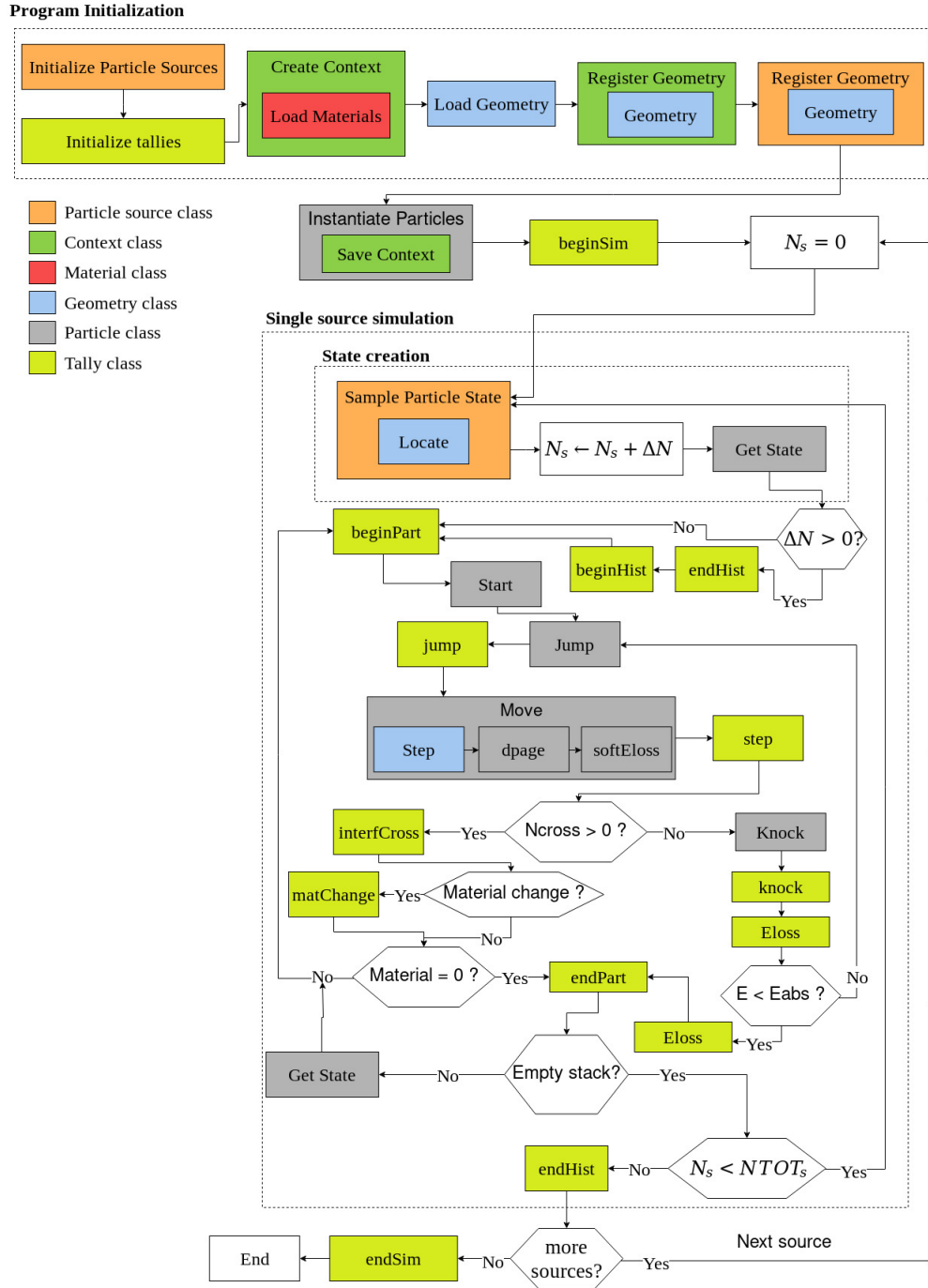


Figure 2: Basic flow diagram of the PenRed main program including tallies. For more details and a complete description of the flow chart, see the text.

- **tally_matChange**: Called when the particle enters a new material.
- **tally_jump**: Called immediately after a call to the *jump* method.
- **tally_knock**: Called immediately after a call to the *knock* method.

Notice that, for the sake of simplicity, the example being discussed here does not include all the possible methods nor does it handle all simulation issues. For example, the positron annihilation or if the source generates a particle in a void region are not considered.

The main idea of this approach is that any user can implement his/her own tally by creating a derived class of the base tally class and implementing the methods listed above. Thus, it is not at all necessary to modify the provided main code and other PenRed components. However, our recommendation is that not all methods should be implemented; implement only those required to tally the desired information to be extracted from the simulation.

4.2. Code system

The PenRed code system avoids dependence on auxiliary libraries and external utilities, except for the DCMTK library. PenRed consists of the components represented in figure 3.

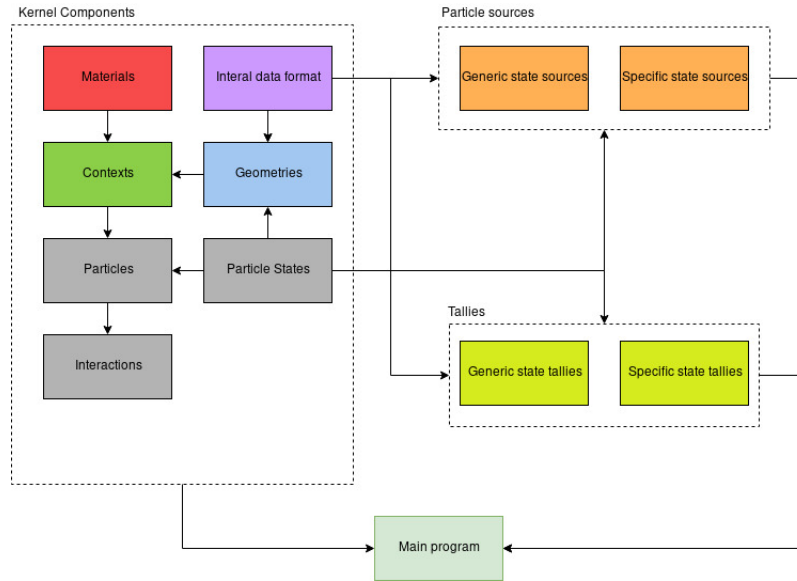


Figure 3: Basic framework components and their dependencies. All components are extensible by creating derived classes and can be integrated with no modification of other components. See the text for details.

All these components can be extended or created via derived classes of the provided abstract classes. In fact, PENELOPE physics and geometries have

been implemented in PenRed using this method. These abstract classes provide the minimum common interface required to ensure that new components are compatible with other PenRed components. In the following subsections, these components are briefly explained. However, a more detailed description is provided in the package documentation.

4.2.1. Kernel components

Kernel components include, by default, the physics and geometries implemented in the original PENELOPE code system. However, the user can extend them by creating new particles, states, material types etc, as shown below. Moreover, PenRed includes a common library to parse configuration data in order to unify input files. The data format adopted in PenRed is similar to the Unix filesystem path representation. For instance, the following lines of a configuration file tell our main program to use a quadric geometry defined in the file `disc.geo`,

```
1 geometry/type "PEN.QUAD"
2 geometry/filename "disc.geo"
```

Listing 1: Internal data format

More examples can be found in the `examples` folder of the PenRed package. Following is a brief description of these components and their function in the PenRed framework.

Particle state

Let us begin with the most basic component, the *particle state*. This component store all the required information to characterise the state and position of a particle in the geometry system. As has been said in section 4.1, the basic particle state includes the following variables,

- **(X,Y,Z)**: Particle position in cm.
- **(U,V,W)**: Direction cosines.
- **E**: Particle energy in eV units.
- **PAGE**: Particle age in seconds.
- **IPAGE**: Flag to control if the particle age must be recorded.
- **WGHT**: Particle weight, which can be modified when variance reduction techniques are used (see section 4.2.4).
- **ILB**: Particle metadata array. This array stores the same information as in the original PENELOPE code.
- **IBODY**: Body index in the geometry system.
- **MAT**: Material index in the geometry system.

If the user needs to store more information for his/her custom particles, we strongly recommend to create a derived class of the provided base particle state. This procedure ensures that the new state will be compatible with existing and future PenRed components. An example of derived state is the used for photons, which includes polarisation information.

Geometries

The next component to consider is the *geometry*, which defines and handles the particle motion across the geometry system. The basic geometry interface requires several auxiliary functions that must be implemented in each new geometry. However, most of these functions are common to similar geometries, for example, body and mesh based geometries. Therefore, to simplify the creation of new geometry types, PenRed provides an extra abstraction layer consisting of two categories: the body and mesh based geometries. Both types are abstract derived classes from the base geometry interface, and provide simplified interfaces to create geometries based on bodies and meshes respectively. Using these middleware classes, the user just needs to implement the *configure*, *step* and *locate* methods, which handle the geometry initialisation, the particle movement and the determination of the body and material indexes at the particle position, respectively. However, the user can implement his/her own geometry component from scratch using the basic geometry interface. One example of a body based geometry implementation can be found in the *pen-quadric* geometry class, which implements the original PENELOPE geometry based on quadrics [7]. For mesh geometries, an example can be found in the *pen-voxelized* geometry class, which implements a geometry formed from a mesh of regular prisms or voxels. It is possible to create a new geometry type combining two or more geometries with the same or different types. For instance, a combined quadric-voxel based geometry can be created, like in PenEasy [49]. It is intended to create a base class for combined geometry types in future versions of PenRed.

Notice that the geometries only use the information provided by the basic particle state, and hence they can be called by any particle class regardless of their state type. It is worth recalling that geometry components should not change their state during the simulation i.e. geometry components must be considered as read only databases. This *soft* requirement is imposed in order to support multi-threading capabilities. Indeed, possible race conditions must be avoided when multiple threads access the same geometry.

Materials and context

Consider now the first read-only component, the *material*. They are intended to store all material specific information, such as mean free paths, absorption energies, density, etc. Therefore, after the initialisation phase, materials are considered as read only databases.

Materials and geometries are stored in a *context*, which serves as a container to integrate together materials, geometry and other auxiliary components or data. When a new context is implemented, a base material type compatible with it must be specified. Nevertheless, this context will be compatible also with

materials derived of, or convertible to, base material types. Consequently, the functionality of existing contexts can be easily extended by creating a derived material with the information required for new interactions or particles. By contrast, the geometry stored in a context can be any of those derived from the basic geometry interface.

Therefore, a context stores all the essential information for particle simulations and, like geometries and materials, serves as a read only database after the initialisation. For this reason, it should not change its state, i.e. the values of its variables, during the simulation. This limitation does not impose a real restriction and allows PenRed to efficiently implement multi-threading capabilities.

Particles

The components described above provide all the needed system and physics information for *particles*. This component requires a context as constructor argument, from which particles will receive all the necessary information to interact with materials and move across the geometry system. This is reason why *particles* are compatible only with a specific context type. However, this compatibility is inherited by derived classes of the base context. Moreover, each *particle* has a base compatible particle state but, as previously, it will also be compatible with derived state types.

The function of the *particles* component is to handle all simulation aspects, like the determination of the step length to the next hard interaction or hinge (*JUMP*), interactions with the corresponding energy loss, angular deflection and production of secondary particles (*KNOCK*), particle soft energy loss along the step, etc. See the documentation for a detailed description of their methods and variables. As mentioned above, PenRed implements the particles used in the original PENELOPE code, i.e. electrons, photons and positrons, including all their physics.

Interactions

Finally, the last kernel component is the *interaction*, which are auxiliary components used to implement particle interactions. They may be avoided because the interactions can be implemented directly within the *KNOCK* and *JUMP* methods. However, the use of *interaction* classes can help the user to create a much cleaner and readable code.

4.2.2. Particle state generators

Particle state generators create the state of initial particles using, generally, a random sampler. In PenRed, the samplers have been divided into the following different types,

- **Spatial samplers:** Perform the sampling of particle position (variables X,Y,Z).
- **Energy samplers:** Sample the initial energy (E).

- **Direction samplers:** Sample the initial particle direction (variables U,V,W).
- **Time samplers:** Set the initial particle age (PAGE).
- **Specific samplers:** Can sample all state variables. This kind of samplers are specific for a particular particle state type. An example is the case of polarised photons, which uses a specific sampler to set the polarisation parameters.

Spatial, energy, direction and time samplers are considered *generic* samplers, because they are common to all particle states. All sampler types have been implemented as independent modules and can be combined with each other. Thus, the user can create a custom spatial sampler and use it with all existing energy, direction, time and specific samplers. On the other hand, specific samplers can be combined with generic ones to delegate partially or totally the generic state creation and handle only a part of the state. Like all other components, samplers should be implemented as derived classes of the corresponding sampler base class. For more information about samplers and how to implement them, see the PenRed package documentation.

4.2.3. Tallies

Tally modules are used to extract information from simulations. To accomplish this task, the tally base class contains a set of virtual methods that are called at specific simulation points to extract the desired information, as seen in section 4.1 and figure 2. Each time a certain event occurs, the associated function is called. The data produced by these events is collected by those tallies which implement the corresponding functions. All tallies are handled by a “cluster” tally class whose function is to wrap simulation tallies and controls the event calls. This class allows to use different tallies and to incorporate new ones with no source code modifications. Therefore, in order to implement a new tally, the user needs to create both the *configure* method and the corresponding event functions required to gather the quantities of interest for the tally. PenRed provides several examples of tallies for different purposes. For instance to measure energy deposition in each material, particle fluence, spatial dose distribution in a mesh of regular prisms or the angular distribution of emerging particles. A detailed description of how to implement new tallies can be found in the PenRed documentation.

Generic tallies access a generic particle state through the argument of the event functions. However, PenRed also implements a special template class for tallies which allows specific particle states to be passed as arguments to the class.

4.2.4. Main program

The PenRed package provides a main program to simulate electrons, photons and positrons which uses all previous components. The functionality of this program can be extended by implementing custom samplers, geometries and tallies that will automatically be available in the main program without changing

a single line of code of the PenRed libraries and the provided main program. The user only needs to include his/her source files and paths in the appropriate files according to the sampler, geometry or tally types. See the PenRed documentation for more information. Nevertheless, in order to add a new particle it is necessary to slightly modify the PenRed main program or create a new one. It is possible to create a generic main program to include new particles, contexts and materials automatically; however, this approach has been avoided to balance performance and flexibility, as described in the next section 4.3.

In addition to PENELOPE physics, PenRed main program implements the very same variance reduction techniques as original Fortran code. These are, for generic simulations, interaction forcing, x-ray and bremsstrahlung splitting. Then, phase space file based simulations adds particle splitting and Russian Roulette techniques. For detailed information refers to the documentation.

4.3. Performance and flexibility

In this section the trade-off between performance and flexibility achieved by the PenRed code is discussed.

As seen in section 4.2, most components must be implemented as derived classes of the corresponding abstract or interface class. Components with compatibility limitations, such as *materials* and *particles*, implement a template class as basic interface to avoid the use of pointers or references to interface classes as arguments in common methods. These templates obtain the compatible base types as template arguments. The motivation to use this approach is to ensure two main features. The first feature is safety because, as compatible types are specified via template arguments, the usage of non compatible types is forbidden. The second one is performance because this approach improves the code performance avoiding the implicit up-cast from derived classes to interface classes and, possibly, some downcast from interface to derived classes. These casts would be executed billions of times, incurring in an unnecessary overhead. Thus, the code flexibility without compromising its performance is maintained.

Another problem to consider is that the usage of virtual methods in interface classes which must be implemented in derived classes, produces a non negligible overhead [50] in functions that are called continuously during a simulation, like the particle *JUMP* and *KNOCK* methods. In order to partially avoid the use of virtual tables during the simulation, *particles*, *contexts*, *materials* and *interactions* are instantiated and utilised through the final derived class and not as a pointer to the abstract base class. Moreover, the statement *final* has been used on critical functions to avoid the use of virtual function tables. To measure the effect of this strategy on the performance of PenRed, a detailed profiling has been carried out in some of the examples provided in the PENELOPE package. In this analysis, the software Valgrind [51] with the Callgrind tool [52], which provide a detailed information about the number of instructions required by each class, function and line of code, have been employed. The most time-consuming functions for both codes (C++ and Fortran) are the particle simulation loops, and, within them, the *JUMP*, *STEP* and *KNOCK* subroutines. The latter represent about 80 – 90% of the simulation loop time in the profiled

examples. For this reason, they have been optimised in PenRed to improve the simulation speed and compensate for losses due to virtual function calls, which make up about 5% of the loop total execution time in some examples. However, this percentage depends strongly on the configuration and geometry of the simulation.

The next issue to be discussed is the presence of global variables and modules in the original Fortran code, which prevents an efficient use of multi-threading parallelization. In the PenRed code, all these global variables have been distributed into the corresponding classes as member variables. Moreover, related variables which are employed together in many computations have been grouped into appropriate structures to improve memory access and cache usage. This technique has been used, for example, in particle states and quadric body and surface definitions.

Taken into account the previous considerations and the code restructuring discussed in section 4.2.1, PenRed fulfils all the prerequisites for implementing an efficient parallelization, as explained further below.

Parallelism

With regard to parallelism capabilities, both the PenRed framework and its provided main program support multi-threading and multi-processing. Multi-threading is implemented by means of standard C++ threads, thus it does not require any non standard library. Furthermore, this kind of parallelism has been implemented to ensure that any new component (tally, particle source, geometry, etc) added to the original package will be automatically compatible with multi-thread executions. The only requirement for tallies is that the user must specify how to sum up the data of two independent tallies by defining the method *sumtally*, which takes a tally of the same type as argument.

The simulation parallelization follows the following procedure. First of all, each thread requires a number of histories to be simulated for each source ($nhists_{th}^s$). This number is calculated from the division of the number of histories to simulate for a given source ($nhists_{total}^s$) by the number of threads ($nthreads$).

$$nhists_{th}^s = \frac{nhists_{total}^s}{nthreads} \quad (2)$$

where the superscript s , specifies the source and the subscript th , is the thread index. Secondly, each thread receives the very same simulation context, a set of unique initial seeds to create a private random generator, a particle source generator and a private tally cluster to retrieve thread-based measures. Once each thread has the necessary data, they will create and simulate its corresponding number of particles to finally sum the results of tallies. It should be remembered that contexts, materials and geometries are read only databases, thus threads can share these components without caring about race conditions. However, other components necessitate a careful study to avoid statistical correlations and race conditions when multiple threads access them.

Regarding random number generators, it has to be assured that each thread follows an independent random number chain. This can be accomplished by assigning the initial seeds by means of the *rand0* routine, which ensures a separation between random chains of 10^{14} . These seeds are provided in the original Fortran package and have been obtained using the program presented in [53].

For particle source generators, special care should be taken to ensure that these components are thread-safe. As explained in section 4.2, there exist two kind of generators, generic and specific. The former are implemented through constant methods by the user. They can be called concurrently because only changes on the particle state and not in the source state itself are permitted. Nevertheless, to allow the implementation of more general sources, specific sources can change their own state. Therefore, for specific sources, the thread-safe condition must be ensured by the programmer.

As regards tallies, each thread has its own and private tally cluster. Therefore, it is completely safe to write on tallies using multiple threads. When the simulation ends, the main thread will add up all tallies using the corresponding *sumtally* functions. The total time needed to sum the tallies is negligible and hence it is not necessary any parallelization on this step. The study and implementation of higher post-processing requirements are left for future work.

In addition to race conditions, the code should avoid the problem of *false sharing* [54]. In PenRed, this effect could occur when certain data is accessed by a thread and another one modifies some data in the same cache block. This would force the first thread to update its cache line even if the accessed value has not changed, what would produce a performance drop due to extra memory accesses. In order to check this effect we have performed a simple test where the code stores the random generators of each thread in a contiguous array. This approach achieves a speed-up of 1.6 with 2 threads. By contrast, the actual code creates the random generators within each thread to avoid false sharing and achieves a speed-up in the range $1.92 - 2.0$, in the same machine and with identical simulation parameters.

Consider now the multi-processing capabilities of PenRed. Multi-processing has been implemented by means of the Message-Passing Interface (MPI) standard to support executions on distributed memory systems, such as node clusters. PenRed MPI implementation is completely compatible with the multi-threading discussed above and can be used together. Taking into account both kinds of parallelism, a generic execution involves np MPI processes, each with nth threads. Accordingly, each MPI process requires a set of random initial seeds to initialise its local threads. PenRed main program assigns a *range* of seeds to each MPI process according to the following rule,

$$[p \cdot nth, (p + 1) \cdot nth] \quad (3)$$

where p is the process identifier or *rank*, and *nth* is the number of threads per MPI process. As with thread history splitting, in an MPI execution the number of histories to be simulated on each MPI process is calculated as,

$$nhists_p^s = \frac{nhists_{total}^s}{np} \quad (4)$$

Therefore, the number of histories to be simulated in each process is divided between the local threads according to equation 2. Subsequently, the program follows the same flow as in the case of multi-threading or single thread simulations, until all partial simulations are completed. After that, the simulation results of each MPI process are stored in the tally cluster corresponding to thread number 0. The final step is to add the partial results of all MPI processes following a binary tree scheme as shown in figure 4. To send tally results between threads, PenRed uses a custom library designed to perform binary *umps* of the state of the simulation. Such a *ump* provides a checkpoint to resume a stopped simulation. Furthermore, this mechanism is used by the MPI post-processing step to transfer the simulation results between processes as binary *umps*. The *ump* is received by the corresponding process, loaded into an auxiliary tally cluster and added to the tally sum by calling the *sumtally* functions, as in multi-threading post-processing.

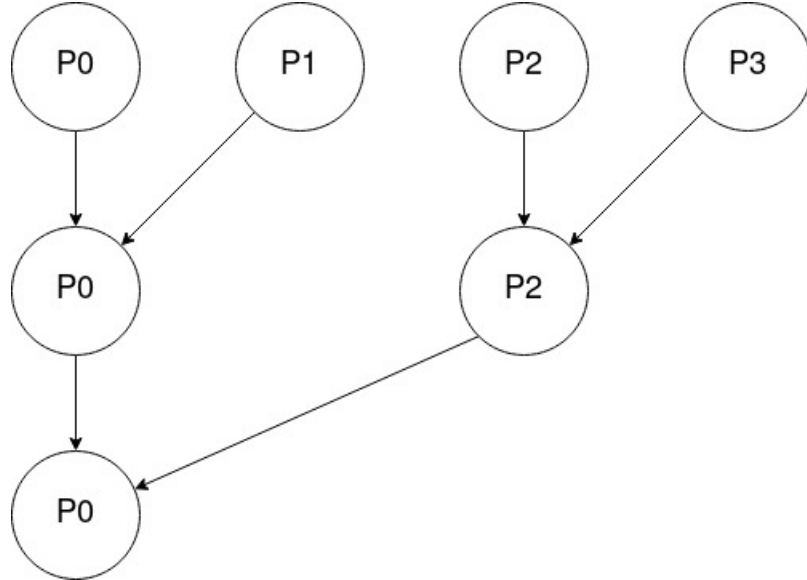


Figure 4: Scheme of the reduce operation used to add the partial simulation results of all MPI processes.

Notice that all the tallies that define the function *sumtally* will automatically be compatible with both kinds of parallelism, multi-threading and MPI. The reason to choose this approach, instead of letting the MPI compatibility to be handled by each tally, is that it produces a negligible overhead in the post-processing step and allows the user to fully exploit the parallelism provided by PenRed in custom modules even without any knowledge of parallel

programming.

Both kinds of parallelism can be enabled or disabled using configuration options in the compilation step which, for example, allows the user to avoid the installation of an MPI implementation.

4.4. *DICOMs*

Besides flexibility and performance, another requirement to perform fast and adaptable Monte Carlo simulations for medical applications is the capability to read and process medical images. These images are usually stored using the international standard of Digital Imaging and Communications in Medicine (DICOM) [55]. This is the standard supported by PenRed, as described below.

To offer support for this image format, PenRed uses the open-source DICOM ToolKit (DCMTK) to extract data from DICOM files. This library can be found in most linux repositories and on github [48]. PenRed implements a DICOM module to read data from DICOM files and a DICOM geometry module to convert it automatically to a voxel geometry, i.e. a 3-dimensional grid formed by tiny parallelepipeds of equal size, ready to simulate. By employing these modules and the provided main program, the user only needs to specify some calibration information and the path to the directory where the DICOM images are stored, to use a DICOM image as a geometry. The tracking algorithm for voxel geometries is based on the PENCT [56] and PenEasy [49] programs.

At the moment, the allowed image modalities are Computed Tomography (CT), Ultrasound (US), Radiotherapy Structure Set (RTSTRUCT) and Radiotherapy Plan (RTPLAN). Since DICOM images can be generated by different types of medical scanners, specific information is needed to perform the conversion from DICOM units to material and density. For example, on CT images, the relationship between Hounsfield units (HU) and density (g/cm^3) is determined by a conversion polynomial whose coefficients should be obtained from a scanner calibration. The user must usually specify density intervals to assign a material for each voxel. However, density and material can be assigned using image contour information which specifies a density and material to one or more DICOM contours. On the other hand, the only way to assign material and densities to US images is via contours. Positron Emission Tomography (PET) images (PT modality) have currently no utility in the PenRed framework. However, in a future version a specific source module designed to convert PET images into spatial particle sources will be included in PenRed.

5. Results

In this section, a collection of tests designed to verify the functionality of the PenRed framework are presented. The tests include checking whether all the results of the examples of the original PENELOPE Fortran code are reproduced, verifying multi-threading capabilities and validating the processing of voxel/DICOM geometries by reproducing a GEANT4 DICOM example.

The results of the MPI tests will not be described here because their conclusions and figures are completely equivalent to those obtained from the multi-threading analysis (see section 5.3). Moreover, as MPI processes communicate between each other only in the post-processing step, and its contribution to the total simulation time is completely negligible, it is useless to discuss a scalability analysis of MPI executions. In fact, the scalability, in simulations with negligible tally sum processing time, is determined by the slowest process and it is approximately “perfect” on a homogeneous cluster.

For the sake of clarity and easy of reading, only the results from a representative subset of the whole set of performed tests will be shown. However, the user can find all the examples with the corresponding materials, geometries and configuration files in the directory `examples` of the distribution package and use them to reproduce our results.

Most of the implemented features for quadric geometries can be validated by performing the following simulations with penmain: **1-disc-vr**, **3-detector** and **5-accelerator-2**. For **1-disc-vr**, the material system defined in the geometry file `disc.geo`, which is represented in figure 5, is a homogeneous copper cylinder whose radius and height can be set by the user in the geometry file. The source is a point-like gun that produces a uniform conical beam of electrons with initial energy 40 keV in the direction of the Z axis with a narrow semi-aperture of 5 degrees specified in the input file `disc.in`. The electrons impact on the cylinder from below. This example has two variants: with and without variance reduction (VR) techniques. The results of the former will be presented below so as to check the PenRed implementation of VR methods.

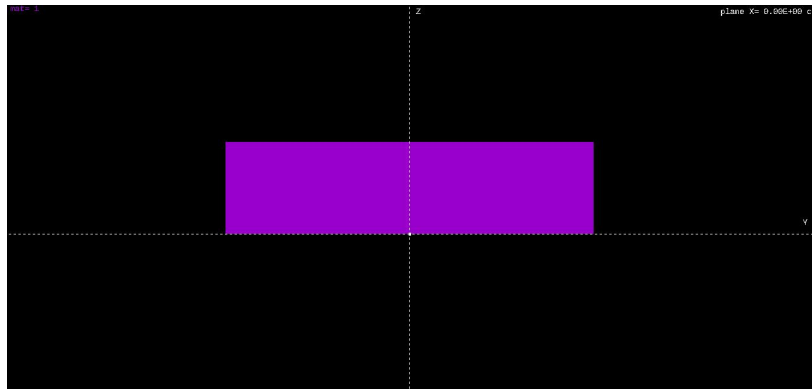


Figure 5: Geometry of the PENELOPE’s **1-disc-vr** simulation example. The viewpoint is along the X axis.

The material system of the example **3-detector**, depicted in figure 6, consists of a 2 in \times 2 in cylindrical NaI scintillator detector with 0.5–inch Fe backing. A point-like Co-60 gamma-ray source emits a photon pencil beam in the $-Z$ direction with equiprobable energies 1.17 and 1.33 MeV. The photons impinge on the NaI crystal from above. No VR is applied in this example.

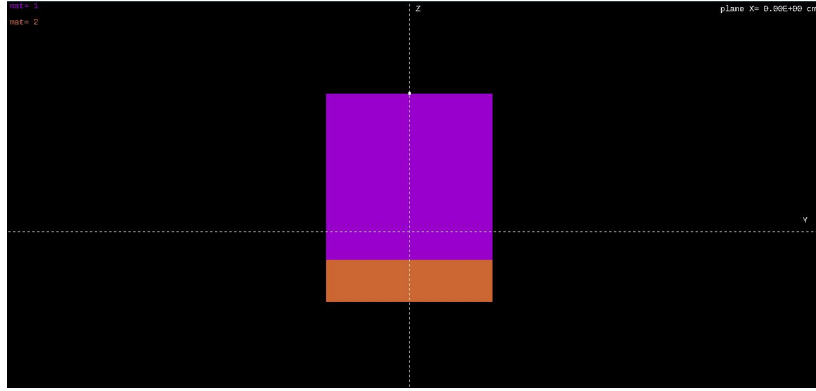


Figure 6: Geometry of the PENELOPE’s 3-detector simulation example. The viewpoint is along the X axis.

Finally, **5-accelerator** simulates a simple electron accelerator and calculates the dose distribution in a water phantom in two steps. In the first step, a phase space file (PSF) is generated at a plane beyond the bottom of the accelerator head. In the second step, **pen_main** reads initial particle states from that PSF and produces the dose distribution in the water phantom. The use of a PSF is of vital importance in medical simulations because it contains a pre-calculated spectrum generated by radioactive seeds and accelerator beams so that different configurations of the same medical treatment can be efficiently simulated. This technique saves huge amounts of computation time in Monte Carlo simulations. However, this kind of simulations requires continuous access to the disk to read the particle spectrum from the PSF, which can cause a significant drop in performance and may affect speed-up or scalability in multi-threading simulations. Therefore, a study of the characteristics of this example is specially interesting. Notice that in most cases the first step, i.e. the creation of the PSF, does not require a huge acceleration because the PSF only needs to be generated once but can be used in multiple simulations. For this reason, in this section we will focus on the second step, the simulation with the pre-calculated PSF.

The material system for the example **5-accelerator** (see figure 7), specified in the geometry file **accelerator.geo**, consists of a simple model of electron accelerator head and a water phantom. The material of the accelerator head is tungsten, the detector volume is filled with air and the material of the phantom is water. The PSF at the exit of the accelerator head is generated using a planar impact detector.

Turning to the validation of the implemented features for voxel geometries, as mentioned in section 4.4, support for these geometries is necessary to perform Monte Carlo simulations using medical images. Basic tests consist of converting quadric geometries to voxel geometries and carrying out the very same simulation on both geometry types. The conversion can be carried out through the provided utility **geo2voxel**, which transforms any geometry into a voxel one

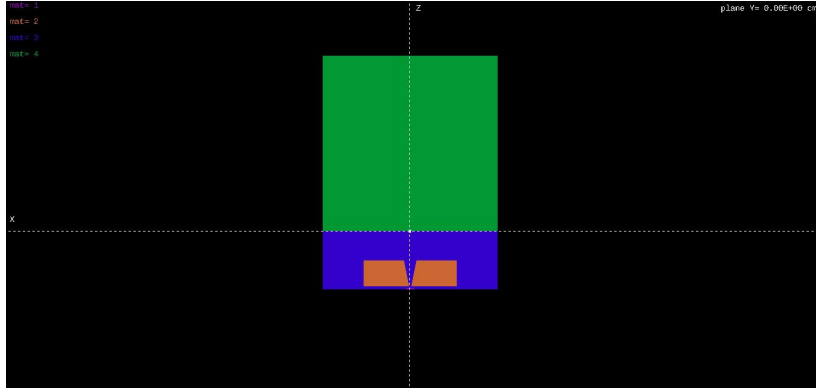


Figure 7: Geometry of the PENELOPE’s 5-accelerator simulation example. The viewpoint is along the Y axis.

by means of the `locate` method. The output file contains a voxel geometry ready to be simulated. We have verified that the results from quadric and voxel geometries are perfectly compatible within statistical error bars. For the purpose of brevity, we will not discuss the results of these tests here. Our results however can be easily reproduced by the user using the tools provided in the package distribution. Instead, a more complete test consisting of a simulation on a DICOM image, is presented in section 5.2.

To run the tests, we used a single node with two Intel(R) Xeon(R) CPU E5-2660 v3 @ 2.60 GHz processors, 8 TB of disk storage and 125 GB of memory RAM. Each of these processors had 10 physical cores with hyper-threading, i.e. a total of 20 physical and 40 logical threads. The PenRed modules and the `pen_main` program were compiled using the `g++` GNU C++ Compiler version 7.3.1 [57], on a Centos 7.0 Linux operating system.

5.1. PENELOPE examples

In order to validate PenRed, the simulation results from all the setups of the examples included in the PENELOPE Fortran package were reproduced. These tests were done using a single thread. The comparison was carried out by plotting all output files for the corresponding tallies and by a bin-by-bin analysis of the differences between PENELOPE and PenRed histograms to ensure that they were statistically compatible. Notice that particle tracks on both programs follow in general different paths, in spite of the fact that both the random generator and initial seeds were the same. The reason is twofold: on the one hand, the differences in the main program structure, such as the use of independent stacks for each particle type in PenRed, and on the other hand, the different round-off errors that occur in the calculation of intersections of particle trajectories with material interfaces. We have verified that the results from PENELOPE and PenRed are perfectly equivalent in all the cases studied

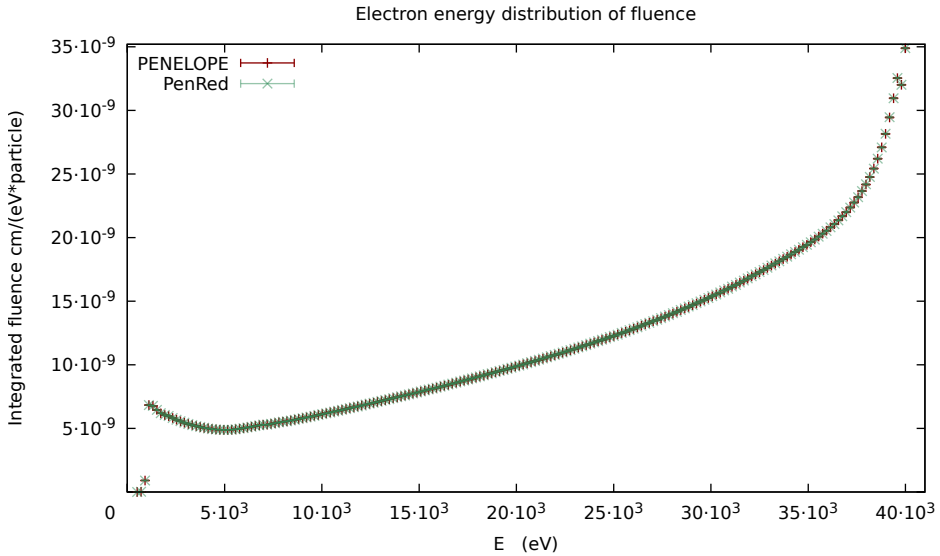


Figure 8: Simulation results of the electron fluence energy distribution integrated over the detector volume of example **1-disc** with variance reduction techniques. The red (dark) colour represents results from the original PENELOPE code, while green (light) points are the results from PenRed. Some transparency to PenRed points is applied because both curves overlap. Error bars enclosure a deviation of 2σ .

and that the differences are usually less than the statistical uncertainties of the data.

In the first example, **1-disc-vr**, interaction forcing techniques were used to increase both the electron bremmstrahlung emission and hard inelastic collision probabilities by a factor 2000 and 200, respectively. In addition, a splitting factor of 2 on bremmstrahlung and x-ray produced photons was applied. The simulation parameters were $E_{abs} = 1$ keV, $C_1 = C_2 = 0.05$ and $W_{cc} = W_{cr} = 1$ keV. The cylinder itself is defined as an energy-deposition, impact and angular detector. The **pen_main** program was run for about 10.9 hours to generate 8×10^6 histories, which corresponds to a simulation speed of about 204 histories per second. Figure 8 displays a comparison between the results from PENELOPE and PenRed of the electron energy distribution of fluence integrated over the detector volume.

Moreover, figure 9 shows another relevant quantity simulated in this example, namely the probability energy distribution of downbound particles, i.e. those that escape from the material system in the negative Z direction, specified by the W variable in particle states. The comparison of the simulation results for the energy distribution of downbound particles is depicted for electrons and photons.

As can be seen from figs. 8 and 9, the results from PENELOPE and PenRed are perfectly compatible within statistical error bars. Moreover, the results are

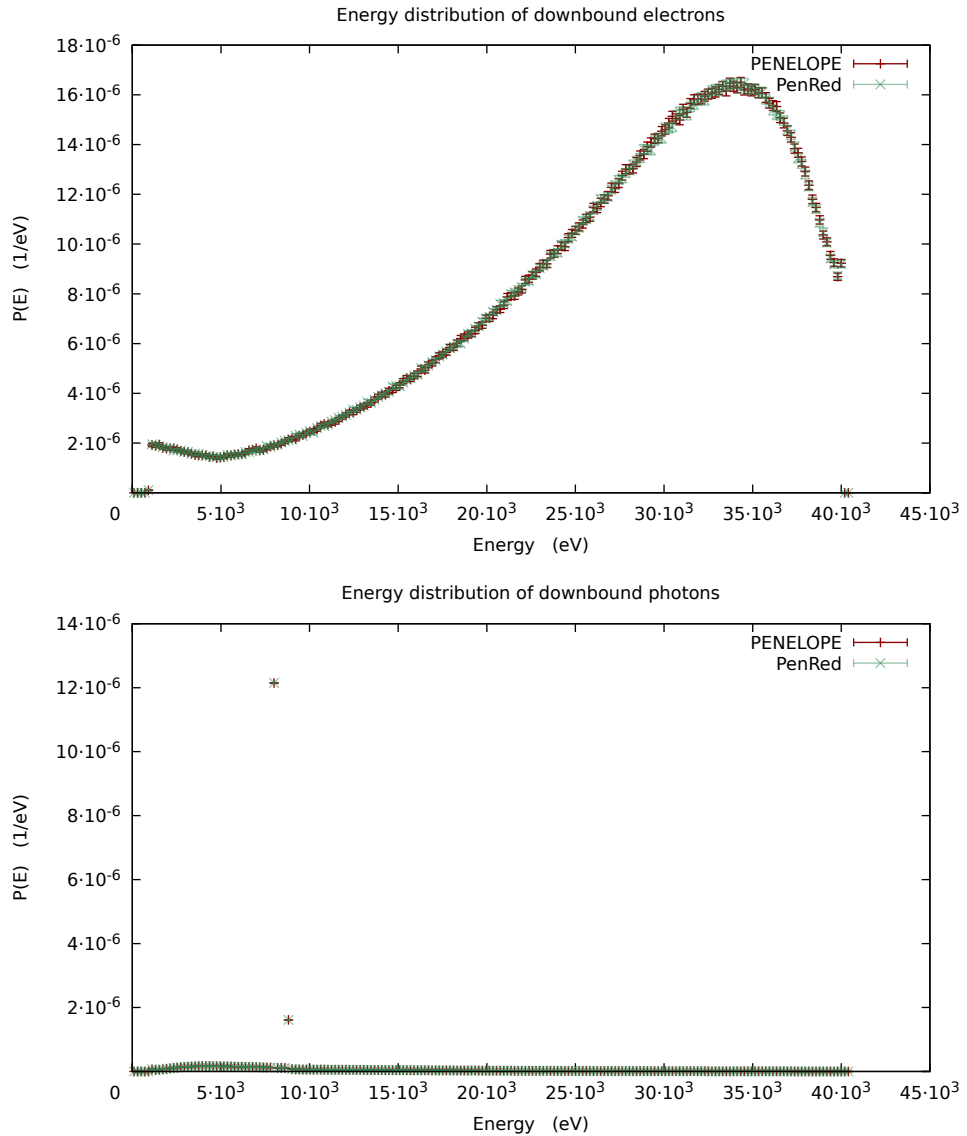


Figure 9: Downbound probability energy distributions for electrons (up) and photons (down) simulated in the example 1-disc using VR techniques. The red (dark) colour represents results from the original PENELOPE code simulations, while green (light) dots are the results from PenRed. For the sake of clarity, some transparency to PenRed points is applied because both curves overlap. Error bars enclosure a deviation of 2σ .

bin-by-bin equivalent with differences that are smaller than statistical errors.

In the example **3-detector**, the simulation parameters were $E_{abs}(e^\pm) = 50$ keV, $E_{abs}(\gamma) = 5$ keV, $C_1 = C_2 = 0.1$ and $W_{cc} = W_{cr} = 2$ keV. The NaI crystal is defined as an energy-deposition detector. The `pen_main` program was run for about 10.6 hours to generate 10^8 histories, which corresponds to a simulation speed of about 2,623 histories per second. Figure 10 displays the comparison of results of this example for the deposition energy spectrum from both codes, PENELOPE and PenRed. Again, as is evident from the figures, both codes produce equivalent results.

In the last PENELOPE example presented here, namely, the **5-accelerator**, the simulation of the PSF previously created in the first step of this test, is performed. The simulation parameters were $E_{abs}(e^\pm) = 100$ keV, $E_{abs}(\gamma) = 10$ keV, $C_1 = C_2 = 0.2$ and $W_{cc} = W_{cr} = 2$ keV, for all materials except for the tungsten slab of the accelerator head for which they were $C_1 = C_2 = 0.1$. The `pen_main` program was run for about 3 hours to generate 2.3×10^6 histories, which corresponds to a simulation speed of about 210 histories per second. In figure 11, the comparison of the results for the depth dose distribution in a water phantom is depicted. As illustrated in this figure, PENELOPE and PenRed are perfectly compatible.

Furthermore, figure 12 displays a comparison between the PENELOPE and PenRed codes of the probability density function (PDF) of the polar angular distribution for emerging electrons and positrons in this example. As can be seen, emerging positrons present huge fluctuations for both codes due to a lower statistics. However, in this case as well both results are compatible within statistical errors.

In addition to the three representative checks discussed above of the correct operation of the PenRed package, some speed tests were performed by running all the examples with both codes as much isolated as possible and using a single thread/process. The programs were run sequentially on the very same processor core employing the `taskset` instruction. PenRed was compiled with `g++ 7.3.1` of GCC [57]. On the other hand, the PENELOPE code was compiled using `gFortran 7.3.1` of GCC. We verified that both codes have very similar simulation speeds for the original PENELOPE examples, despite the extra overhead introduced in PenRed to achieve a flexible and extensible code (see section 4.3).

5.2. DICOM test

As mentioned in section 4.4, a necessary requirement to perform Monte Carlo simulations based on medical images is to automatise the reading and processing of DICOM images. In order to validate the DICOM processing capabilities of PenRed, the DICOM example of GEANT4 was reproduced. This example, included in the GEANT4 distribution package since version 10.4, can be found in the directory `share/Geant4-10.5.1/examples/extended/medical/DICOM` and `DICOM2` of the installation tree of the GEANT4 10.05.p01. In the DICOM extended example, a set of DICOM files are read using a custom internal DICOM reader and converted to simple text files, where the Hounsfield numbers are translated into materials and densities. A GEANT4 geometry is then created

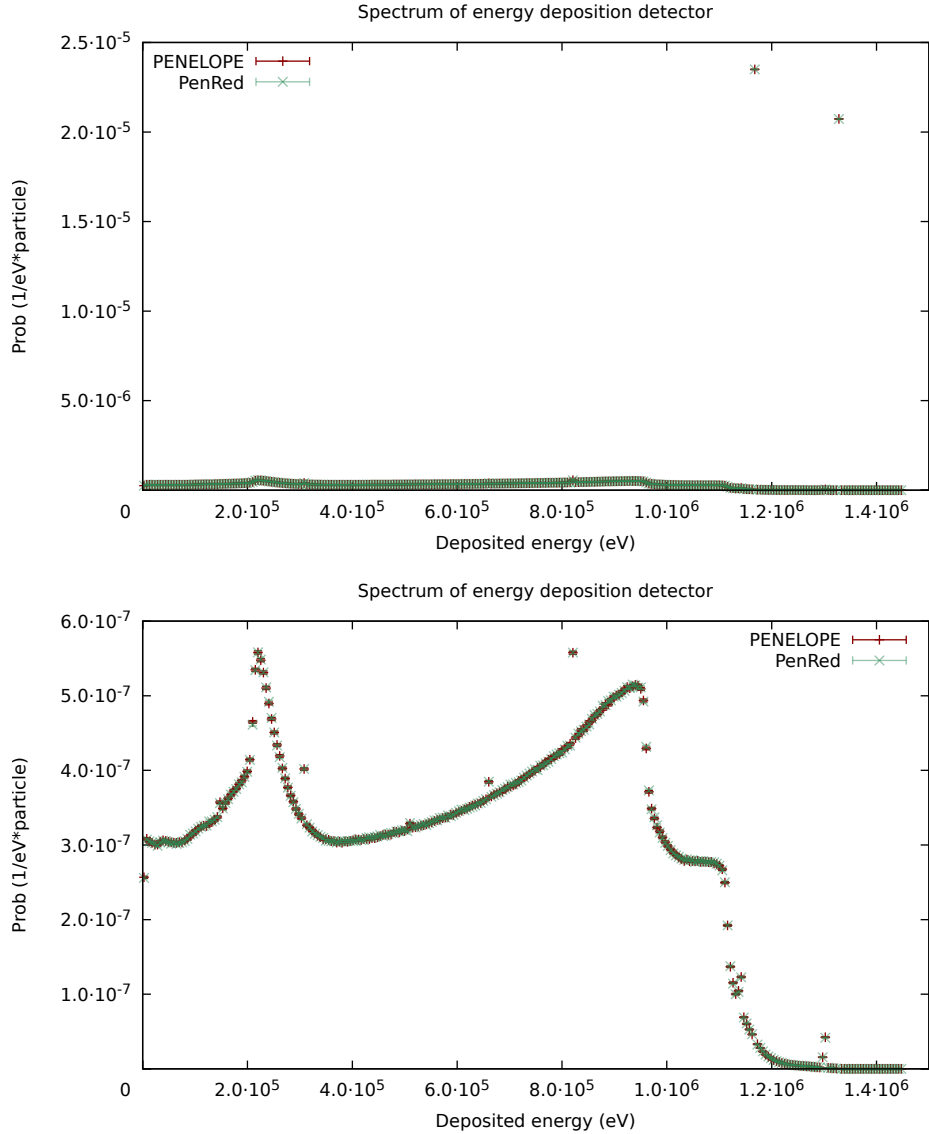


Figure 10: Energy deposition spectrum in a Na scintillator simulation (example 3-detector). The top image shows the complete spectrum, while the bottom image displays the same data but in a smaller probability interval on the Y axis ($[0, 6 \cdot 10^{-7}]$). The colour red (dark) represents results from the original PENELOPE code, while green (light) dots are the results from PenRed. For the sake of clarity, some transparency to the PenRed points is applied because both curves overlap. Error bars enclosure a deviation of 2σ .

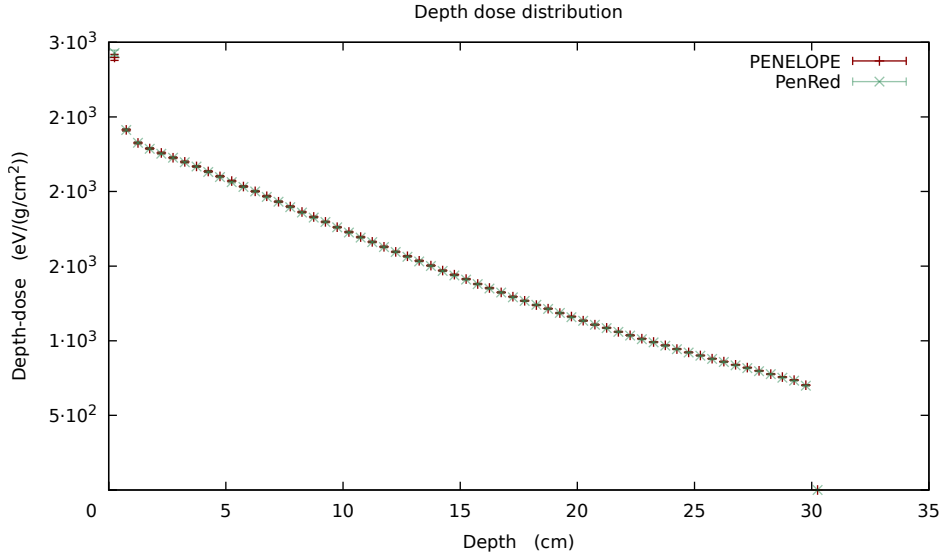


Figure 11: Depth dose distribution along the water phantom corresponding to the second step of the example 5-accelerator. The red (dark) colour represents results from the original PENELOPE code, and the green (light) dots are results from PenRed. For the sake of clarity, some transparency is applied to PenRed points because both curves overlap. Error bars enclosure a deviation of 2σ .

based on the DICOM file information using the `G4PhantomParameterisation`. Finally, a Monte Carlo simulation can be performed on this geometry by choosing one of the different ways of navigation in regular voxelised volumes available in GEANT4. The default and fastest navigation option, `G4RegularNavigation`, was used in this study. The resulting deposited dose voxel distribution is saved in the file `dicom.out` in Gy. For further details, the reader is referred to the GEANT4 documentation [58].

The simulations carried out in these tests were based on the digital head phantom of the DICOM_HEAD project documented in [59]. This project consists of 128 high resolution DICOM files and it is distributed with the other GEANT4 data files on the GEANT4 download site. However, for the reasons explained below, the DICOM_HEAD_TEST subset was used which consists of four DICOM images extracted from the DICOM HEAD project: `60_dicom_125mm`, `61_dicom_125mm`, `62_dicom_125mm` and `63_dicom_125mm`, one Z slice per file. The slice locations are -81.25 , -82.5 , -83.75 and -85 mm, respectively. The number of voxels/pixels in X , Y and Z in each DICOM file is $1024 \times 1024 \times 1$ with dimensions X, Y, Z of $0.1875 \times 0.1875 \times 1.25$ mm. Eight materials are defined: `Air`, with density $\rho = 0.10$ gr/cm 3 , `SoftTissue`, with $\rho = 1.02$ gr/cm 3 , `BrainTissue`, with $\rho = 1.06$ gr/cm 3 , `SpinalDisc`, with $\rho = 1.12$ gr/cm 3 , `TrabecularBone`, with $\rho = 1.40$ gr/cm 3 , `CorticalBone`, with $\rho = 2.0$ gr/cm 3 , `ToothDentin`, with $\rho = 2.5$ gr/cm 3 , and `ToothEnamel`, with $\rho = 3.0$ gr/cm 3 . The conversion of

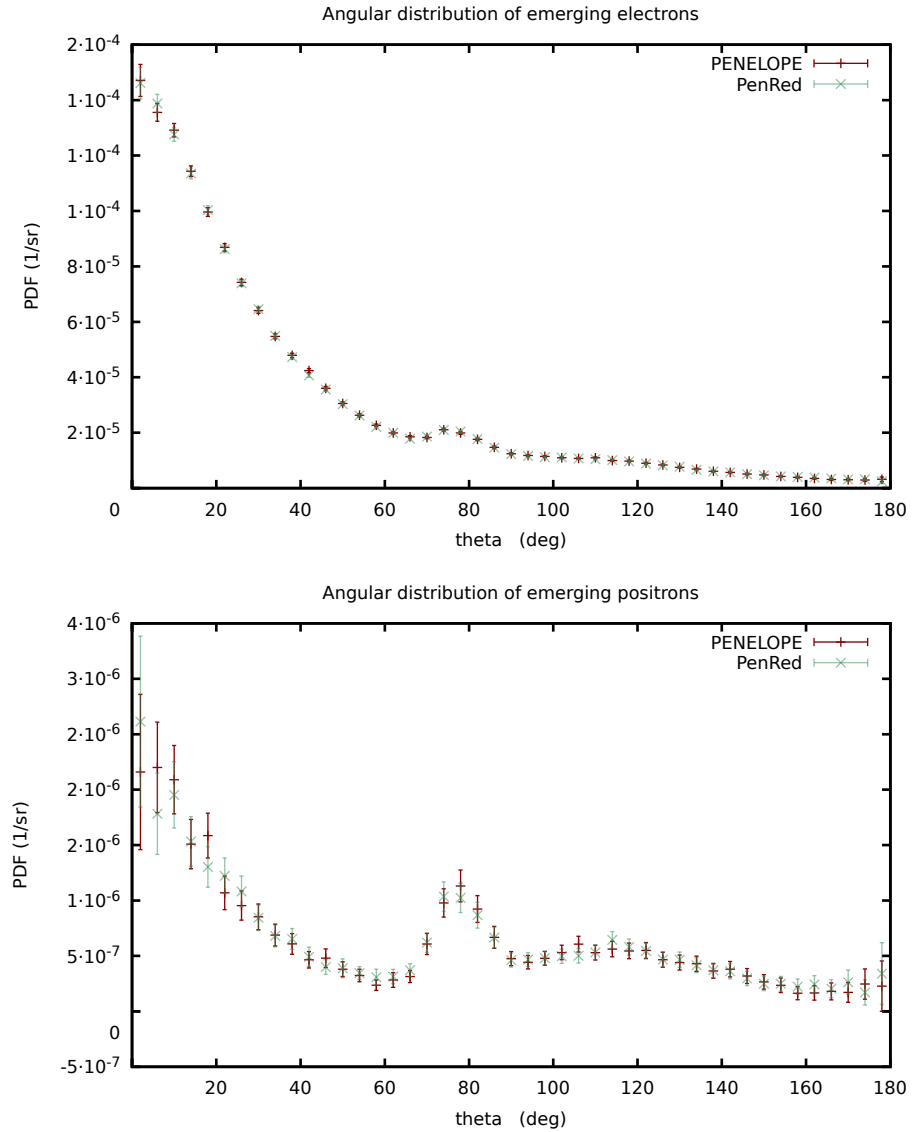


Figure 12: Polar angular distribution of emerging electrons (top) and positrons (bottom) simulated in the second step (PSF simulation) of the example **5-accelerator**. The red (dark) colour represents results from the original PENELOPE code, while the green (light) dots are the results of PenRed. For the sake of clarity, some transparency to PenRed points is applied because both curves overlap. Error bars enclosure a deviation of 2σ .

Hounsfield numbers to materials is not used with the DICOM_HEAD project [59]. The material is associated to the voxel in the Detector Construction, in the case of GEANT4, and directly in the input file in the case of PenRed, without using a calibration curve.

The test consisted in comparing the simulation results for the distribution of absorbed dose from GEANT4 and PenRed. Notice that the GEANT4 uses a different random number generator which can introduce some differences of statistical nature between results from GEANT4 and PenRed.

The procedure used to simulate with PenRed follows. Firstly, using the provided program `material`, the necessary materials were created according to their compositions and densities described in the GEANT4 DICOM example code. After that, the `pen_main` program was run to simulate a 100 MeV monoenergetic electron beam emitted from a point-like source located at the point $(0, 0, -120)$ mm with initial direction along the positive Z axis, $(0, 0, 1)$. As advised by the authors, this simulation is extremely slow. They recommend to use few slices and a low number of histories. Following his/her recommendations, we simulated 10^8 histories with only the four DICOM slices described above with both codes, GEANT4 and PenRed. The simulations were performed running the DICOM and `pen_main` programs, respectively, in multi-threaded mode with 20 threads on the infrastructure specified in section 5. In addition, in order to improve the simulation speed, both codes were compiled with the Intel C++ compiler (`icc`) version 19.0.5.281 [60] (see section 5.4 for further details).

The total absorbed dose obtained with GEANT4 was 342.29 Gy, to be compared to 341.055 Gy with a standard deviation of $2\sigma = 0.553$ Gy, from PenRed. As can be seen, they are compatible with a relative difference of about 0.3%. Moreover, we verified that the distributions of the absorbed dose from both codes were also equivalent. A high statistics simulation of this setup was also performed by running only the PenRed code. The program was run on 40 threads for about 14.5 hours to generate 10^{10} histories, which corresponds to a simulation speed of about 191,800 histories per second. In figure 13, the absorbed dose distribution maps for the four slices of the DICOM_HEAD_TEST data set are shown. The result for the total absorbed dose was 341.063 Gy with $2\sigma = 0.063$ Gy, perfectly compatible with the above low statistics result.

5.3. Multi-threading tests

In this section, the validation of the multi-threading operation of PenRed is discussed. The same tests with the same simulation parameters, computer setup and compiler options as those presented in section 5.1, were carried out by running the PenRed `pen_main` program on a single thread and on 5 threads so as to compare the results. The data of each pair of the corresponding output files was compared bin by bin against each other. Figure 14 shows some results for the detector example (3-detector).

All comparisons carried out showed that the results from a single thread and multiple thread simulations are statistically compatible. Therefore, we can ensure that our multi-threading program works properly. In order to repro-

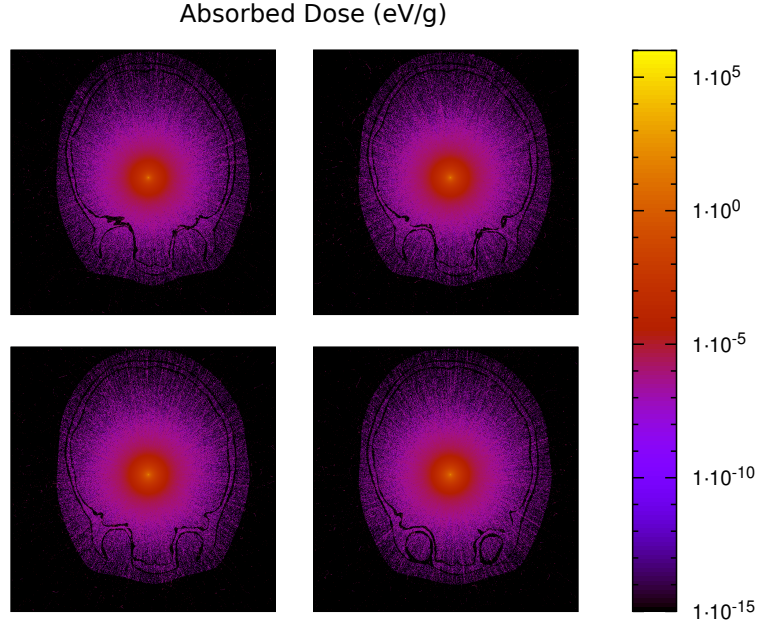


Figure 13: Absorbed dose distribution maps on the four slices of the DICOM_HEAD_TEST data set. The top slice located at -81.25 mm corresponds to the left top corner image. The next slices located at -82.5 and -83.75 mm are the top right and bottom left images, respectively. The bottom slice located at -85 mm corresponds to the bottom right image.

duce our results, the user only needs to change the parameter $nthreads$ in the provided input configuration files of any of the examples.

In the rest of this section, the speed-up and scalability of the PenRed framework in multi thread runs is studied. To measure the speed-up, the quantity S_n is used. It is defined as

$$S_n = \frac{time_n}{time_1} \quad (5)$$

where the subscript n indicates the number of threads, $time_1$ is the simulation time using a single thread and $time_n$ the simulation time using n threads. Ideally, S_n should tend to the number of threads n , which is the maximum speed-up that can be achieved.

The same three representative examples as in section 5.1 were used in this analysis. Due to the fact that the reading of phase space files involves frequent disk accesses, a worse speed-up for the example **5-accelerator** was expected.

However, we found that all of the tested examples show a similar speed-up behaviour. In figure 15, the values of S_n as a function of the number of threads are presented for the examples **1-disc** and second step of **5-accelerator**. Similar results were obtain for the example **3-detector**. The green lines represent linear fits to the measured speed-up data when a maximum of one thread was

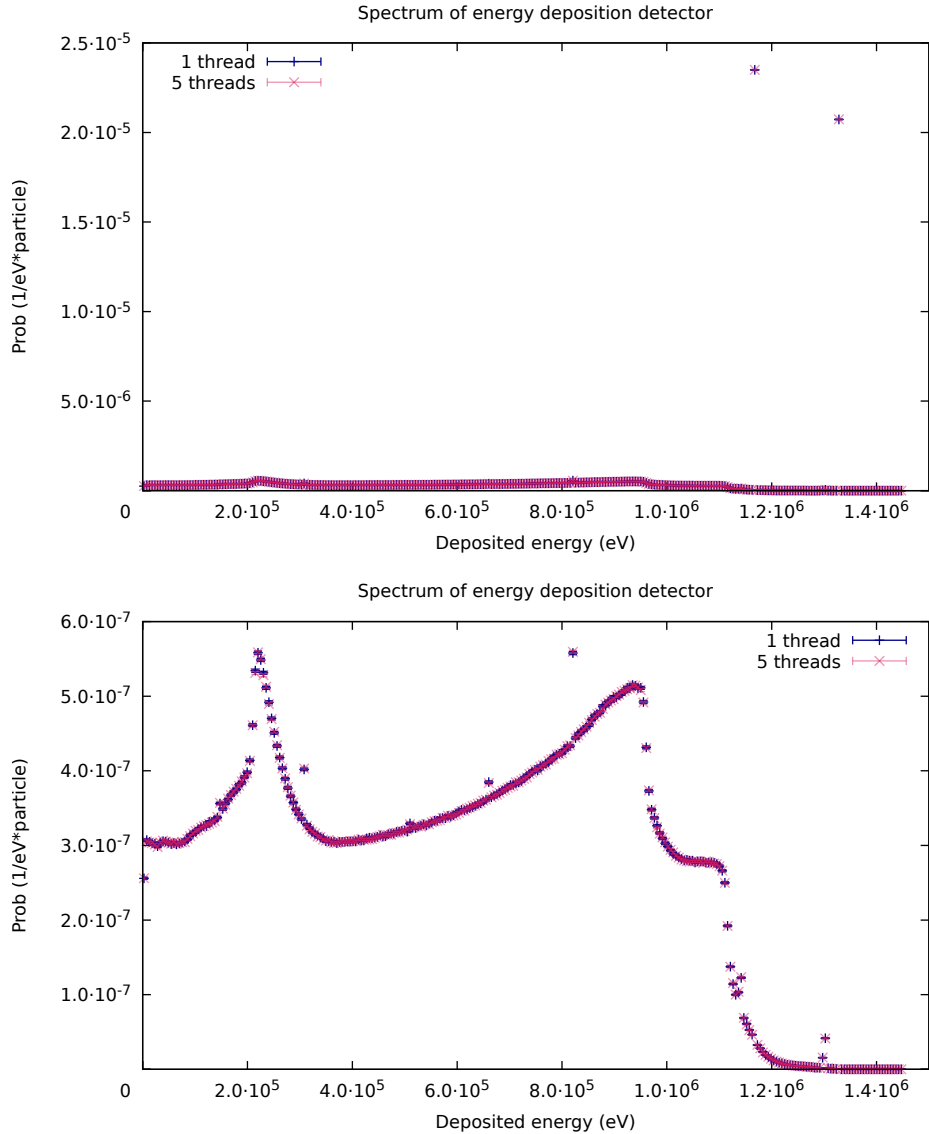


Figure 14: Energy deposition spectrum in a *Na* scintillator simulation (example 3-detector). The top image shows the complete spectrum, while the bottom image displays the same data but in a smaller probability interval on the Y axis ($[0, 6 \cdot 10^{-7}]$). The colour blue (dark) represents results from single thread simulations, while purple (light) are the results from runs on 5 threads. For the sake of clarity, some transparency to the points corresponding to the runs on 5 threads is applied because both curves overlap. Error bars enclosure a deviation of 2σ .

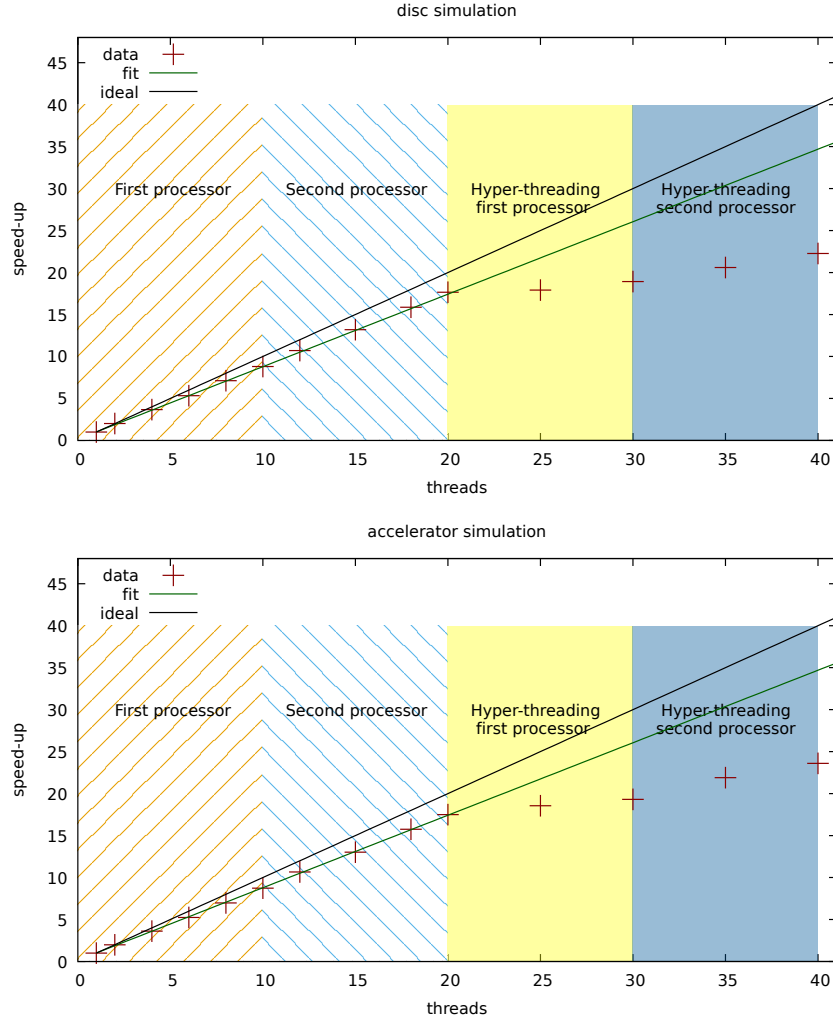


Figure 15: Speed-up values for examples 1-disc (top) and the second step of 5-accelerator (bottom). Graphs are divided into four zones. The zone hatched with right-oblique lines on the interval between 1 and 10 threads corresponds to the first processor, while that hatched with left-oblique lines on the interval between 11 and 20 is associated to the second processor. Therefore, for no more than 20 threads, the processors do not use hyper-threading capabilities. Solid yellow (light) and blue (dark) zones correspond to logical threads for the first and second processors, respectively, for which hyper-threading is active. The black line represents a perfect ideal speed-up while the green line is a linear fit to the speed-up data from 20 threads or less.

executed on each physical processor core, corresponding to the zone between 1 and 20 threads. In this zone, as processors do not use hyper-threading capabilities, a linear correlation between speed-up and the number of used threads was obtained.

The slopes of the linear fits are 0.87 and 0.86 for the disk and accelerator examples, respectively. Thus, PenRed achieves a similar speed-up even when the process needs to read information from disk storage during the simulation. This is because PSF reads have been optimised in PenRed by loading chunks of particles instead of one particle at a time. Furthermore, the time required to read the whole PSF is negligible as compared with the duration of the simulation which, however, depends strongly on the simulation parameters and geometry.

5.4. Performance tests

To maximise the program efficiency, the speed-up tests were repeated using the Intel C++ compiler [60] (`icc`) version 19.0.5.281. We found that tests performed by running on a single thread the code compiled with `icc` are faster (about 50-60%), as can be seen in table 5.4. Furthermore, PenRed compiled with `icc` has a slightly higher speed-up on multi-threading. The speed-up behaviour and graphs are very similar to those in section 5.3, but their slopes in the linear region are slightly better. Indeed, for the examples of the disc and the second step of accelerator, these slopes are 0.89 and 0.88 respectively.

Example	GCC	icc	Increase (%)
1-disc-vr	$2.037 \cdot 10^2$	$3.039 \cdot 10^2$	49.16
3-detector	$2.623 \cdot 10^3$	$4.167 \cdot 10^3$	58.88
5-accelerator	$2.097 \cdot 10^2$	$3.194 \cdot 10^2$	52.31

Table 2: Comparison between simulation speeds (histories/s) using the very same code compiled with GNU `g++` version 7.3.1 and Intel `icc` version 19.0.5.281. Both codes have been run on the same computer setup with a single thread. The first column specifies the example tested. The second and third columns contain the simulation speed in histories per second for the code compiled with `g++` and `icc`, respectively. Finally, the last column shows the increase in the simulation speed in percentage.

6. Conclusions and future work

PenRed provides a flexible, object-oriented, parallel and general purpose framework for Monte Carlo simulations of radiation transport in matter based on PENELOPE physics. These features have been achieved without compromising simulation speed. PenRed includes all the PENELOPE physics models and it has been thoroughly tested that PenRed reproduces within statistical errors the results from the complete set of PENELOPE examples. In addition, our code system includes support to simulate voxel geometries and DICOM images, which make it suitable for performing Monte Carlo simulations of medical treatments. Moreover, our results can be reproduced by the user using the input files provided in the PenRed package.

Regarding parallelism, PenRed incorporates a mixed model for handling both distributed and shared memory parallelism via MPI standard and the standard C++ thread library, respectively. Both types of parallelism achieve good speed-ups even with simulations that use phase space files, widely used for example in brachytherapy and external beam treatments.

Furthermore, the modular structure of PenRed allows the developer to incorporate new custom components (particle sources, geometries, tallies, etc.) which can be included with no modifications in other PenRed components. The new components will be automatically usable in parallel computations without any previous knowledge of parallel programming.

In future versions of PenRed, we plan to create a load balance module to take advantage of heterogeneous architectures, to implement new tallies and sources for medical applications, and, thanks to its modular structure, to adapt PenRed to perform generic simulations on specific hardware accelerators, such as GPGPUs and FPGAs.

Acknowledgements

The authors are deeply indebted to F. Salvat for many comments and suggestions, for clarifying many subtleties of the simulation algorithms of the transport of particles through matter, specially using PENELOPE, and for his patience and understanding. The work of V. Gimenez-Alventosa was supported by the program “Ayudas para la contratación de personal investigador en formación de carácter predoctoral, programa VALi+d” under grant number ACIF/2018/148 from the Conselleria d’Educació of the Generalitat Valenciana and the “Fondo Social Europeo” (FSE). V. Gimenez acknowledges partial support from FEDER/MCIyU-AEI under grant FPA2017-84543-P, by the Severo Ochoa Excellence Program under grant SEV-2014-0398 and by Generalitat Valenciana through the project PROMETEO/2019/087.

References

- [1] F. Salvat, Åsa Carlsson Tedgren, Jean-François Carrier, Stephen D. Davis, Firas Mourtada, Mark J. Rivard, Rowan M. Thomson, Frank Verhaegen, Todd A. Wareing, Jeffrey F. Williamson, Report of the task group 186 on model-based dose calculation methods in brachytherapy beyond the tg-43 formalism: Current status and recommendations for clinical implementation, *Med. Phys.*
- [2] M. J. Rivard, B. M. Coursey, L. A. DeWerd, W. F. Hanson, M. S. Huq, G. S. Ibbott, M. G. Mitch, R. Nath, and J. F. Williamson, Update of aapm task group no. 43 report: A revised aapm protocol for brachytherapy dose calculations, *Med. Phys.*

- [3] National cancer institute, <https://seer.cancer.gov>, accessed: 2019-09-30.
- [4] Salvat F., Penelope. a code system for monte carlo simulation of electron and photon transport, Issy-Les-Moulineaux: OECD Nuclear Energy Agency.
- [5] PenRed, <https://github.com/PenRed>, accessed: 2020-02-13.
- [6] J. Baró, J. Sempau, J. M. Fernández-Varea, and F. Salvat, PENELOPE: An algorithm for Monte Carlo simulation of the penetration and energy loss of electrons and positrons in matter, *Nucl. Instrum. Meth. B* 100 (1995) 31–46.
- [7] F. Salvat, PENELOPE-2018: A code System for Monte Carlo Simulation of Electron and Photon Transport, OECD/NEA Data Bank, Issy-les-Moulineaux, France, 2019, available from <http://www.nea.fr/lists/penelope.html>.
- [8] GEANT4 Collaboration (Agostinelli. S. et al.), Geant4: A simulation toolkit, *Nucl.Instrum.Meth. A*506 250-303 SLAC-PUB-9350, FERMILAB-PUB-03-339.
- [9] EGSnrc: software tool to model radiation transport, <https://github.com/nrc-cnrc/EGSnrc>, accessed: 2017-07-2.
- [10] H. Hirayama, Y. Namito, A. F. Bielajew, S. J. Wilderman, W. R. Nelson, The EGS5 Code System, *Tech. Rep. SLAC-R-730* (KEK 2005-8), Stanford Linear Accelerator Center, Menlo Park, California (2006).
- [11] I. Kawrakow, E. Mainegra-Hing, D. W. O. Rogers, F. Tessier, B. R. B. Walters, The EGSnrc Code System: Monte Carlo Simulation of Electron and Photon Transport, NRCC Report PIRS-701, National Research Council Canada, Ottawa, CAN, 2019.
- [12] Los Alamos Scientific Laboratory. Group X-6., Mcnp : a general monte carlo code for neutron and photon transport. los alamos, n.m., Dept. of Energy, Los Alamos Scientific Laboratory.
- [13] A. Ferrari, P. R. Sala, A. Fassò, J. Ranft, FLUKA: A multi-particle transport code (program version 2005), *CERN Yellow Reports: Monographs*, CERN, Geneva, 2005. doi:10.5170/CERN-2005-010.
URL <https://cds.cern.ch/record/898301>
- [14] J. Sempau, J. M. Fernández-Varea, E. Acosta, and F. Salvat, Experimental benchmarks of the Monte Carlo code PENELOPE, *Nucl. Instrum. Meth. B* 207 (2003) 107–123.
- [15] F. Salvat, J. M. Fernandez-Varea, Overview of physical interaction models for photon and electron transport used in monte carlo codes, *Metrologia* 46. doi:10.1088/0026-1394/46/2/S08.

- [16] F. Salvat, A. Jablonski, C. J. Powell, ELSEPA—Dirac partial-wave calculation of elastic scattering of electrons and positrons by atoms, positive ions and molecules, *Computer Physics Communications* 165 (2) (2005) 157–190. [doi:10.1016/j.cpc.2004.09.006](https://doi.org/10.1016/j.cpc.2004.09.006).
- [17] ICRU Report 77, *Elastic Scattering of Electrons and Positrons*, ICRU, Bethesda, MD, 2007.
- [18] D. Liljequist, Simple calculation of inelastic mean free path and stopping power for 50 eV-50 keV electrons in solids, *J. Phys. D; (United Kingdom)* 16.
- [19] R. M. Sternheimer, The density effect for the ionization loss in various materials, *Phys. Rev.* 88 (1952) 851–859.
- [20] M. J. Berger, M. Inokuti, H. H. Anderson, H. Bichsel, J. A. Dennis, D. Powers, S. M. Seltzer, J. E. Turner, Stopping powers for electrons and positrons, Report 37, *Journal of the International Commission on Radiation Units and Measurements* 19.
- [21] D. Bote, F. Salvat, Calculations of inner-shell ionization by electron impact with the distorted-wave and plane-wave born approximations, *Phys. Rev. A* 77 (2008) 042701. [doi:10.1103/PhysRevA.77.042701](https://doi.org/10.1103/PhysRevA.77.042701)
URL <https://link.aps.org/doi/10.1103/PhysRevA.77.042701>
- [22] X. Llovet, Powell, J. Cedric, F. Salvat, A. Jablonski, Cross sections for inner-shell ionization by electron impact, *Physical and Chemical Reference Data* 43 (2014) 013102.
- [23] S. M. Seltzer, M. J. Berger, Bremsstrahlung spectra from electron interactions with screened atomic nuclei and orbital electrons, *Nuclear Instruments and Methods in Physics Research Section B: Beam Interactions with Materials and Atoms* 12 (1985) 95–134.
- [24] S. M. Seltzer, M. J. Berger, Bremsstrahlung energy spectra from electron with kinetic energy 1 keV-10 GeV incident on screened nuclei and orbital electrons of neutral atoms with Z=1-100, *At. Data Nucl. Data Tables* 35 (1986) 345–418.
- [25] E. Acosta, X. Llovet, F. Salvat, Monte carlo simulation of bremsstrahlung emission by electrons, *Appl. Phys. Lett.* 80 (2002) 3228–3230.
- [26] A. Poskus, BREMS: A program for calculating spectra and angular distributions of bremsstrahlung at electron energies less than 3 MeV, *Computer Physics Communications* 232 (2018) 237–255.
- [27] W. Heitler, *The Quantum Theory of Radiation*, Oxford University Press, 1954.

- [28] D. T. Cromer, D. Liberman, Relativistic Calculation of Anomalous Scattering Factors for X Rays, *The Journal of Chemical Physics* 53 (1970) 1891–1898.
- [29] D. E. Cullen, J. H. Hubbell, L. Kissel, EPDL97 The Evaluated Data Library, 097 Version, UCRL-50400, Lawrence Livermore National Laboratory, 1997.
- [30] D. Brusa, G. Stutz, J. A. Riveros, J. M. Fernández-Varea, and F. Salvat, Fast sampling algorithm for the simulation of photon compton scattering, *Nucl. Instrum. Meth. A* 379 (1996) 167–175.
- [31] L. Sabbatucci and F. Salvat, Theory and calculation of the atomic photoeffect”, *Rad. Phys. Chem.* 121 (2016) 122–140.
- [32] R. H. Pratt, H. K. Tseng, Behavior of electron wave functions near the atomic nucleus and normalization screening theory in the atomic photoeffect, *Physical Rev. A* 5 (1972) 1063–1072.
- [33] M. J. Berger, J. S. Coursey, M. A. Zucker and J. Chang, Stopping-power and range tables for electrons, protons and helium ions, Tech. rep., Institute of Standards and Technology, Gaithersburg, MD. Available from <http://www.nist.gov/pml/data/star/index.cfm>, 2005.
- [34] S. Perkins, D. Cullen, M. Chen, J. Rathkopf, J. Scofield, J. Hubbell, Tables and Graphs of Atomic Subshell and Relaxation Data Derived from the LLNL Evaluated Atomic Data Library (EADL), Z = 1–100, Vol. UCRL-50400 vol.30, US Department of Energy, Office of Scientific and Technical Information, United States, 1991.
- [35] R. D. Deslattes, E. G. Kessler, P. Indelicato, L. de Billy, E. Lindroth, J. Anton, X-ray transition energies: new approach to a comprehensive evaluation, *Rev. Mod. Phys.* 75 (2003) 35–99. doi:10.1103/RevModPhys.75.35.

URL <https://link.aps.org/doi/10.1103/RevModPhys.75.35>
- [36] J. A. Bearden, X-ray wavelengths, *Rev. Mod. Phys.* 39 (1967) 78–124. doi:10.1103/RevModPhys.39.78.

URL <https://link.aps.org/doi/10.1103/RevModPhys.39.78>
- [37] A. J. Walker, An efficient method for generating discrete random variables with general distributions, *ACM Trans. Math. Software* 3 (1977) 253–256.
- [38] Martin J. Berger, Monte Carlo calculation of the penetration and diffusion of fast charged particles, in: B. Alder, S. Fernbach, M. Rotenberg (Eds.), *Methods in Computational Physics*, Vol. 1, Academic Press, New York, 1963, pp. 135–215.
- [39] H. W. Lewis, Multiple scattering in an infinite medium, *Phys. Rev.* 78 (1950) 526–529.

[40] I. Kawrakow, D. W. O. Rogers, The EGSnrc code system: Monte Carlo simulation of electron and photon transport, Tech. Rep. PIRS-701, National Research Council of Canada, Ottawa (2001).

[41] J. M. Fernández-Varea, R. Mayol, J. Baró, F. Salvat, On the theory and simulation of multiple elastic scattering of electrons, *Nucl. Instrum. Meth. B* 73 (1993) 447–473.

[42] F. Salvat, Class II algorithm for charged particle transport simulation, Private communication.

[43] S. Goudsmit, J. L. Saunderson, Multiple scattering of electrons, *Phys. Rev.* 57 (1940) 24–29.

[44] S. Goudsmit, J. L. Saunderson, Multiple scattering of electrons. II, *Phys. Rev.* 58 (1940) 36–42.

[45] G. Molière, Theorie der Streuung schneller geladener Teilchen II: Mehrfach- und Vielfachstreuung, *Z. Naturforsch. 3a* (1948) 78–97.

[46] L. D. Landau, On the energy loss of fast particles by ionization, *Journal of Physics-USSR* 8 (1944) 201–205.

[47] T. Williams, C. Kelley, many others, Gnuplot 4.4: an interactive plotting program, <http://gnuplot.sourceforge.net/> (March 2010).

[48] DCMTK, <https://github.com/DCMTK/dcmtk>, accessed: 2019-09-28.

[49] J. Sempau, A. Badal and L. Brualla, A PENELOPE-based system for the automated Monte Carlo simulation of clinacs and voxelized geometries—application to far-from-axis fields, *Med. Phys.* 38 (2011) 5887–5895.
URL <http://dx.doi.org/10.1118/1.3643029>

[50] K. Driesen, U. Hölzle, The direct cost of virtual function calls in c++, *SIGPLAN Not.* 31 (10) (1996) 306–323. doi:10.1145/236338.236369.
URL <http://doi.acm.org/10.1145/236338.236369>

[51] N. Nethercote, J. Seward, Valgrind: A framework for heavyweight dynamic binary instrumentation, *SIGPLAN Not.* 42 (6) (2007) 89–100. doi:10.1145/1273442.1250746.
URL <http://doi.acm.org/10.1145/1273442.1250746>

[52] J. Weidendorfer, M. Kowarschik, C. Trinitis, A tool suite for simulation based analysis of memory access behavior, in: M. Bubak, G. D. van Albada, P. M. A. Sloot, J. Dongarra (Eds.), *Computational Science - ICCS 2004*, Springer Berlin Heidelberg, Berlin, Heidelberg, 2004, pp. 440–447.

[53] A. Badal, J. Sempau, A package of linux scripts for the parallelization of monte carlo simulations, *Computer Physics Communications* 175 (6) (2006) 440 – 450. doi:<https://doi.org/10.1016/j.cpc.2006.05.009>.
URL <http://www.sciencedirect.com/science/article/pii/S001046550600230X>

[54] W. J. Bolosky, M. L. Scott, False sharing and its effect on shared memory performance, in: USENIX Systems on USENIX Experiences with Distributed and Multiprocessor Systems - Volume 4, Sedms'93, USENIX Association, Berkeley, CA, USA, 1993, pp. 3–3.
 URL <http://dl.acm.org/citation.cfm?id=1295480.1295483>

[55] DICOM, <https://www.dicomstandard.org/>, accessed: 2019-09-28.

[56] F. Salvat, PENCT: a program for the simulation of electron-photon transport in voxelised structures using PENELOPE, Private communication.

[57] GCC, <https://gcc.gnu.org/>, accessed: 2019-09-2.

[58] Dicom extended example, <https://twiki.cern.ch/twiki/bin/view/Geant4/G4extendedExampleDICOM>, accessed: 2019-09-10.

[59] V. Giacometti, S. Guatelli, M. Bazalova-Carter, A. Rosenfeld, R. Schulte, Development of a high resolution voxelised head phantom for medical physics applications, *Physica Medica* 33 (2017) 182 – 188.
 doi:<https://doi.org/10.1016/j.ejmp.2017.01.007>.
 URL <http://www.sciencedirect.com/science/article/pii/S1120179717300078>

[60] Intel C++ compiler, <https://software.intel.com/en-us/cpp-compiler-developer-guide-and-reference-introducing-the-intel-c-compiler>, accessed: 2019-09-2.